ACTIVE FAULTING AT THE NORTHEAST MARGIN OF THE GREATER PUGET LOWLAND: A PALEOSEISMIC AND MAGNETIC-ANOMALY STUDY OF THE KENDALL FAULT SCARP, WHATCOM COUNTY, NORTHWEST WASHINGTON

By

Elizabeth Anne Barnett

A Thesis

Presented to

The Faculty of Humboldt State University

In Partial Fulfillment

of the Requirements for the Degree

Master of Science

In Environmental Systems: Geology

(May, 2007)

ACTIVE FAULTING AT THE NORTHEAST MARGIN OF THE GREATER PUGET LOWLAND: A PALEOSEISMIC AND MAGNETIC-ANOMALY STUDY OF THE KENDALL FAULT SCARP, WHATCOM COUNTY, NORTHWEST WASHINGTON

by

Elizabeth Anne Barnett

Approved by the Master's Thesis Committee:

Harvey M. Kelsey, Major Professor Date

Mark A. Hemphill-Haley, Committee Member Date

Brian L. Sherrod, Committee Member Date

Elizabeth R. Schermer, Committee Member Date

Sharon L. Brown, Graduate Coordinator Date

Chris A. Hopper, Interim Dean Date
of Research, Graduate Studies & International Programs

ABSTRACT

Active Faulting at the Northeast Margin of the Greater Puget Lowland: A Paleoseismic and Magnetic-Anomaly Study of the Kendall Fault Scarp, Whatcom County, Northwest Washington

Elizabeth Anne Barnett

LiDAR mapping reveals a prominent, 4 km long, south-side up fault scarp that occurs along trend and within 500 m of the Boulder Creek fault in the North Fork Nooksack River valley. Thrust faulting of Late Pleistocene glacial outwash over Holocene soils produced the east-west trending fault scarp. Each time the fault scarp rose, streams flowing south into the Nooksack River ponded along it to form a wetland. Trench and wetland stratigraphy demonstrates a minimum of three late Holocene earthquakes produced the fault scarp. The earliest earthquake generated a fold scarp, followed by two surface-rupturing earthquakes to produce a combined vertical offset of at least two meters. Based on Mazama ash found above the lowest buried wetland soil, the folding event occurred shortly before ~7700 yr BP. Dated organic material from wetland and trench buried soils indicates ages of ~3000 yr BP and ~900 yr BP for the two surface-rupture events.

The record of late Holocene earthquakes that produced the Kendall fault scarp demonstrates that Puget Sound seismic hazard assessments must now consider surface rupturing events and associated ground motion potential in the Bellingham area. Furthermore, the northern limit of north-south compression in western Washington, previously considered to be the Devils Mountain fault zone ~60 km to the south, should now be expanded northward to include active faulting in the Nooksack River valley.

The active faulting may be along an active strand of the previously mapped Boulder Creek normal fault. The opposing sense of displacement, north-side up on the Boulder Creek fault and south-side up on the Kendall fault scarp, may reflect recent reactivation of the Boulder Creek fault as a north-verging thrust fault. Both the fault and fault scarp straddle a significant aeromagnetic anomaly; we test whether they are structurally related by analyzing aeromagnetic and magnetic ground survey data. Analyses of aeromagnetic data, however, do not provide direct evidence of the recent reverse motion recorded in the trenches but may suggest the location of the Boulder Creek fault hidden beneath a thick glacial outwash cover.

ACKNOWLEDGEMENTS AND DEDICATION

I am very much obliged to my thesis advisor, Harvey Kelsey, for his support, encouragement, and mentoring starting with the inception of my project, to field work and analyses, and final thesis editing stages. Furthermore, I learned a great deal about both science and professional character by working with Harvey, and also Brian Sherrod and Craig Weaver of the U.S. Geological Survey (Seattle), whom I thank for steering me toward Humboldt, encouraging me to take on this project, and for their continued generous support. I am also grateful to my other committee members, Mark Hemphill-Haley (Humboldt State University) and Elizabeth Schermer (Western Washington University) for their constructive comments that improved the final draft and illuminating discussions in the trenches (Liz). Richard Blakely of the USGS Menlo Park office entertained my notions of collecting magnetic data and was very generous with his time both collecting and analyzing the data with me. My thanks to Jonathan Hughes (University College of the Fraser Valley) who kindly shared much of the wetland data and acquainted me with gyttja and the business of coring. Ralph Haugerud (USGS Seattle) introduced me to the Kendall fault scarp LiDAR and provided an excellent structural geology background of the Kendall region. I am also very grateful for his GIS tutelage (and for hiring me in the first place). Many thanks to the Puget Sound Lidar Consortium and Tim Hyatt, working for the Nooksack Tribe, who provided the LiDAR data.

The Humboldt faculty and fellow grad students offered me a first rate graduate education, and I thank them for my brief but enjoyable and enlightening experience at HSU. As always, I am indebted to the professional and logistical support I received from the USGS Seattle office, Tom Yelin, Karen Meagher, and Bob Norris, in particular. Nancy Rountree (USGS, Menlo Park) kept everything on the financial end running smoothly. I also thank The Glen and Ferndale Gravel of Maple Falls for access to the study sites.

Finally, I wholeheartedly thank Seth Cowdery, 5212 ½ Ravenna, and my Seattle friends for putting up with my Arcata-Seattle jet-setting and for plying me with excellent adventures, conversation, and chocolate when needed.

My efforts of this project are dedicated to:

my mom, Lucy G. Barnett,

and to the memory of two earth scientists who influenced me greatly:

my dad,

Dr. Stockton G. Barnett

and

Dr. Tony Qamar

TABLE OF CONTENTS

LIST OF TABLES

LIST OF FIGURES

INTRODUCTION

Evidence of recent earthquake-triggered ground surface rupture remained unrecognized in the northeastern Puget Sound until discovery of the Kendall fault scarp near Bellingham, Washington (Haugerud, et al., 2005). During the late Holocene, a minimum of three reverse faulting events created a prominent, east-west trending, 4 km long fault scarp that traverses a glacial outwash terrace along the North Fork Nooksack River. Due to its close proximity to the previously mapped Boulder Creek fault, the fault scarp may be the surface expression of an active strand within a Boulder Creek fault zone.

An analysis of the earthquake history and faulting characteristics that produced the Kendall fault scarp would provide a basis to assess seismic hazards and improve regional tectonic models. Accordingly, the objectives of this study are the following: investigate the earthquake history of the Kendall fault scarp using trench and wetland coring data, characterize the scarp within the context of the regional bedrock and Quaternary geology, and test the idea that the Kendall fault is structurally related to the nearby previously mapped Boulder Creek fault in order to understand its relation to the regional tectonic framework.

PREVIOUS WORK: REGIONAL GEOLOGY AND TECTONIC SETTING

Active shallow faults of the Puget Sound region accommodate north-south shortening in the Cascadia forearc. Oblique, northeast-directed subduction of the Juan de Fuca plate beneath North America provides the driving forces that rotate the Oregon Coast block clockwise; subsequent translation of the Oregon block drives northwestern Washington against the British Columbia Coast Mountains backstop (Fig. 1) (Wells et al., 1998). North-south contraction in the Puget Sound region by 3-3.5 mm/yr (Mazzotti, et al., 2002), or as much as 6-9 mm/yr (Wells et al., 1998; Hyndman et al., 2003), produces active east-west and northwest-southeast trending faults in the Puget Sound region (Fig. 2). Late Holocene paleoseismic histories for several of these Puget Sound faults emerged from investigations of deformed shorelines, marsh subsidence and uplift, wetland inundation, and fault scarps; several of these studies are outlined below.

The Seattle uplift encompasses most of the Seattle urban area (Fig. 2) and is bounded by two active fault zones: the south-dipping Seattle fault zone to the north (Bucknam et al., 1992; Pratt et al., 1997; Johnson et al., 1999; Blakely et al., 2002; Nelson et al., 2003; Brocher et al., 2004) and the north-dipping Tacoma fault zone to the south (Sherrod et al., 2004). Although the Seattle fault zone is a north-verging structure, trench excavations of LiDAR-identified (Light Detection And Ranging) scarps reveal south-verging reverse faults within its leading edge (Nelson et al., 2003). To explain this package of faults with opposite thrust direction, Brocher et al. (2004) propose a passive-roof duplex model for the leading edge of the Seattle uplift with south-verging Holocene

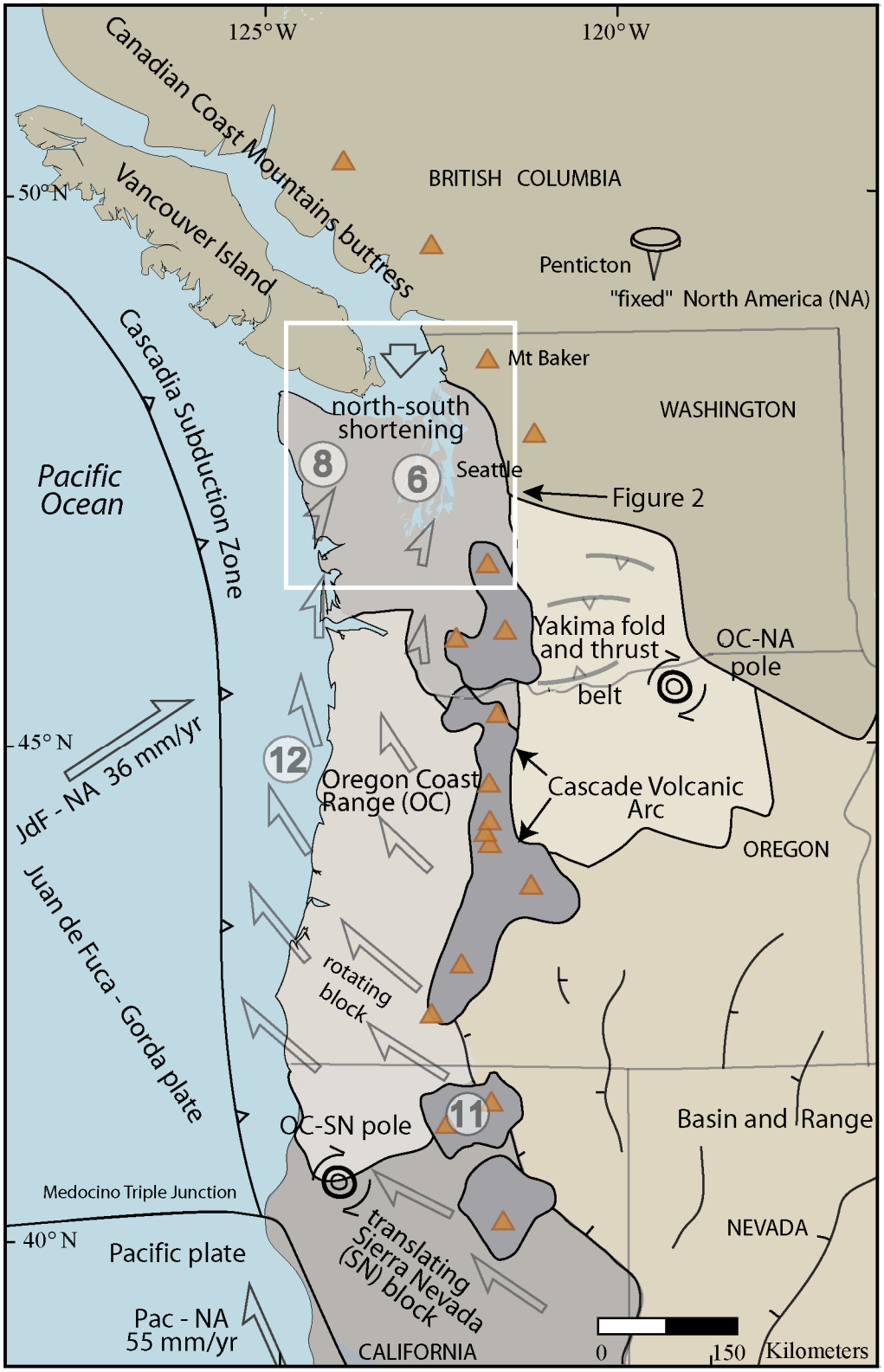

Figure 1: Tectonic block model of Cascadia forearc terranes, after Wells and Simpson (2001) and Wells et al. (1998). Velocity field is shown by arrows. Plate motion (circled numbers) is in mm/yr. The translation of the Sierra Nevada block and rotation of the Oregon Coast Range block about their respective Euler poles induce north-south shortening of western Washington against the Canadian Coast Mountains buttress. Triangles are Cascade volcanoes.

Figure 2: Map of Puget Sound crustal faults. Teeth on up-thrown block. Orange, Holocene-active faults. Black, faults of uncertain activity. Fault sources: Wilson et al. (1979), Johnson et al. (1996), Walsh et al. (1997), Johnson et al. (1999), Tabor et al. (2000), Johnson et al. (2001), Sherrod (2001), Haugerud et al. (2003), Lidke et al. (2003), Nelson et al. (2003), Blakely et al. (2004), Johnson et al. (2004), Kelsey et al. (2004), Sherrod et al. (2004), Witter et al. (2006), Haugerud (written communication, 2006).

thrusts that splay upward from a shallow roof thrust that overlies a north-verging floor thrust.

Paleoseismic studies indicate that thrust faults in both roof and floor positions of the Seattle fault zone have slipped during the late Holocene: trench studies show three earthquakes occurred on reverse splay faults of the Seattle fault zone during the last 2500 years (Nelson et al., 2003), and wave-cut platform (Bucknam et al., 1992), marsh (Sherrod, 2000), and tsunami studies indicate that the last earthquake on the Seattle fault zone created a regional uplift in A.D. 900-930 (Atwater and Moore, 1992). Deformed shorelines that straddle the Tacoma fault (Fig. 2) also record regional uplift between A.D. 770 and 1160 along the southern edge of the Seattle uplift (Sherrod et al., 2004).

North of the Seattle fault zone, the Southern Whidbey Island fault zone crosscuts central and northern Puget Sound (Fig. 2) as a set of strike-slip fault strands with reverse components of displacement (Johnson, et al., 1996). Seismic-reflection studies show that the Southern Whidbey Island fault zone traverses southeast from Victoria, B.C., crosses Puget Sound and Whidbey Island, and strikes land near Everett (Johnson et al., 1996). The southeasterly trace of the Southern Whidbey Island fault zone then trends toward the Cascade Mountains northeast of Seattle, as shown by aeromagnetic anomaly and trench studies of LiDAR-identified scarps (Blakely et al., 2004). Similar to Seattle uplift faults, paleoseismic evidence indicates Holocene earthquake activity along the Southern Whidbey Island fault zone. Whidbey Island sea-level history studies by Kelsey et al. (2004) suggest that the last earthquake occurred approximately 3000 yr BP.

Previously considered the northern limit of north-south compression, the Devils Mountain, Utsalady Point and Strawberry Point faults (Fig. 2) are elements of an oblique slip transpressional deformation zone between southern Vancouver Island and the Cascade foothills (Johnson et al., 2001; Johnson et al., 2004). The earthquake history of this system is not well understood; however, trench investigations of fault scarps suggest that the Utsalady Point fault ruptured at least once, and possibly twice, during the late Holocene (Johnson et al., 2004).

No scarps representing Holocene earthquakes were identified in the Puget Sound north of the Devils Mountain fault until discovery of the Kendall fault scarp (Fig.2). Consequently, the results of this study suggest that the northern zone of active Puget Sound crustal faults should be expanded north to include the Kendall fault and the northeastern margin of the Puget Sound.

GEOLOGY, GEOPHYSICS, AND LANDSCAPE OF THE KENDALL FAULT SCARP STUDY SITE

Located at the intersection of the Puget lowland, the Fraser River lowland, and the foothills of the North Cascades Mountains, the Kendall fault scarp traverses a landscape constructed by terrane accretion and remolded by glaciers (Fig. 3). Outwash from the last glaciation both reveals recent earthquake activity and conceals deeper fault structures: outwash is offset by recent faulting, producing the Kendall fault scarp, and blankets the Boulder Creek bedrock fault mapped nearby. Boulder Creek fault subsurface expression may be indicated by the contrasting magnetic signatures of rocks separated by the fault that produce magnetic anomalies. A striking anomaly straddles both the Boulder Creek fault and the Kendall fault scarp.

Stuctural Geologic Setting

The North Cascade foothills surrounding the Kendall fault scarp are situated within the Northwest Cascade System, an assemblage of imbricated fault-bounded blocks of metamorphosed Late Paleozoic to Mesozoic oceanic and volcanic sedimentary rocks. During Late Cretaceous time these rocks were accreted to North America (Misch, 1966; Misch, 1977; Brown et al., 1987; Tabor et al., 1994; Tabor et al., 2003). Following accretion, the Northwest Cascade System rocks were cut by Eocene high angle strike-slip and normal faults and blanketed by thick sedimentary deposits of Chuckanut Formation (Brown, 1987). One such high angle fault within the Kendall fault scarp area is the north-side-up, normal Boulder Creek fault. This fault and the Smith Creek fault separate

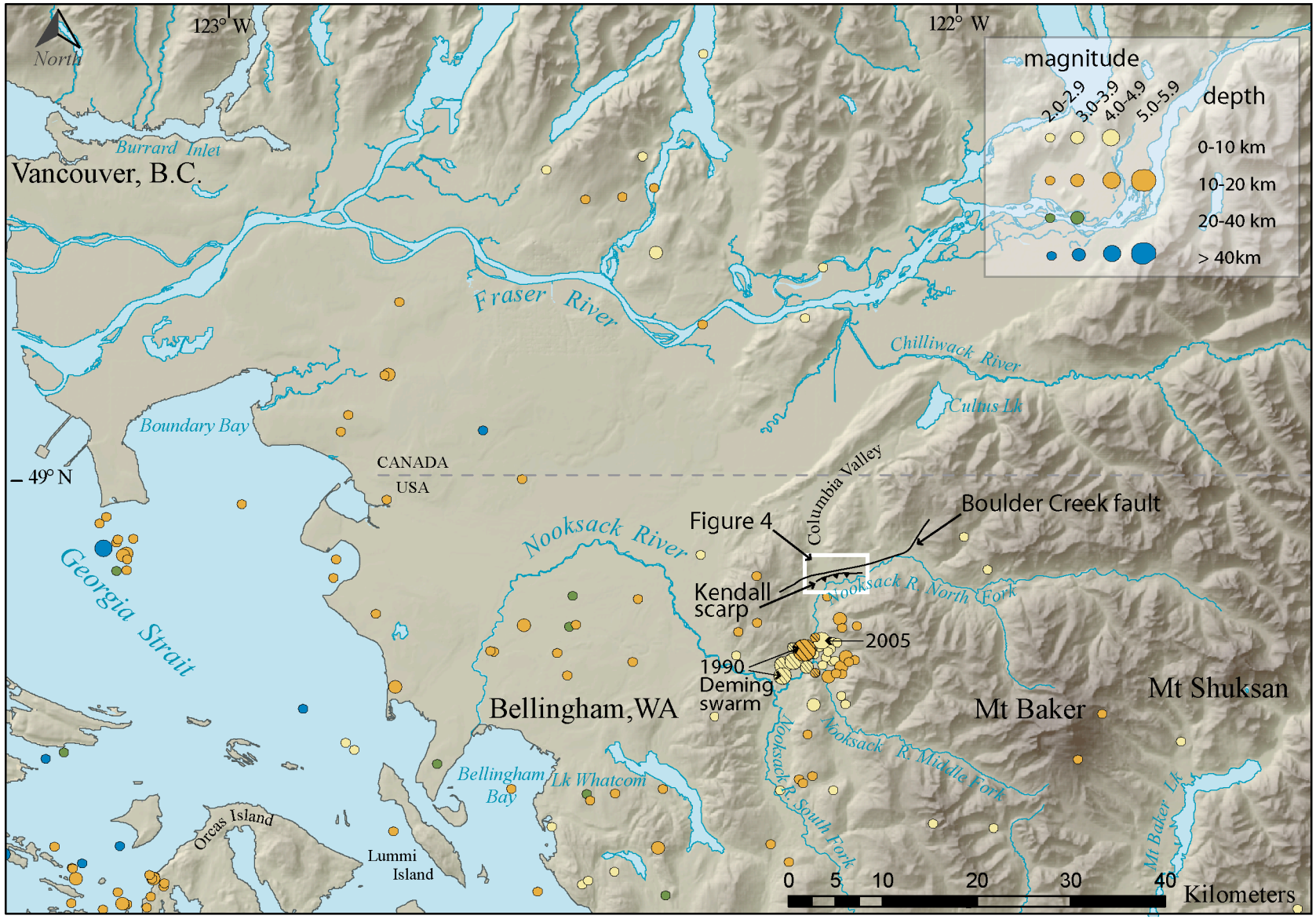

Figure 3: Map of Nooksack River drainage area including Kendall scarp and Boulder Creek Fault. Earthquakes dates are from Pacific Northwest Seismic Network, 1969-2006. The 1990 Deming swarm earthquakes labeled with diagonal hatched lines.

Chilliwack Group/Bell Pass Melange (pT) to the north from the Chuckanut Formation (Tc) to the south (Fig. 4) (Moen, 1962; Dragovich et al., 1997a; Tabor et al., 2003; Haugerud, written communication, 2006). The inclusion of locally-derived Chilliwack/Bell Pass Melange clasts within the Eocene-Oligocene Maple Falls Member of the Chuckanut Formation (which composes the bedrock hill immediately west of the Kendall fault scarp trench locations) provides evidence that the Boulder Creek fault may have been active in the Eocene as Chuckanut sediment was being deposited and faulted (Johnson, 1982; Dragovich et al. 1997a). Johnson (1982) suggests that the Boulder Creek and Smith Creek faults form the north and west boundaries of an Eocene pull-apart basin during an extensional event, after which faulting activity on the Boulder Creek fault probably ceased.

Magnetic Signature of Faulted Rocks

The Boulder Creek and Smith Creek faults separate regions of high and low magnetic anomalies (Fig. 5) (Blakely et al., 1999). Pre-Tertiary rocks north and west of the Boulder Creek fault and Smith Creek fault show the highest magnetic intensities while Chuckanut Formation rocks in the down-faulted basin are relatively magnetically quiet. The exception is the prominent magnetic anomaly that straddles the Boulder Creek fault and the Kendall fault scarp, shown in the center of Figure 5. The most magnetic rocks near the faults appear to be within, or possibly below, the Huntingdon Formation (outlined in green in Fig. 5), the Bell Pass Melange serpentine-rich rocks (pTu) on Sumas Mountain (outlined in yellow in Fig. 5), and Chilliwack Group volcaniclastic rocks

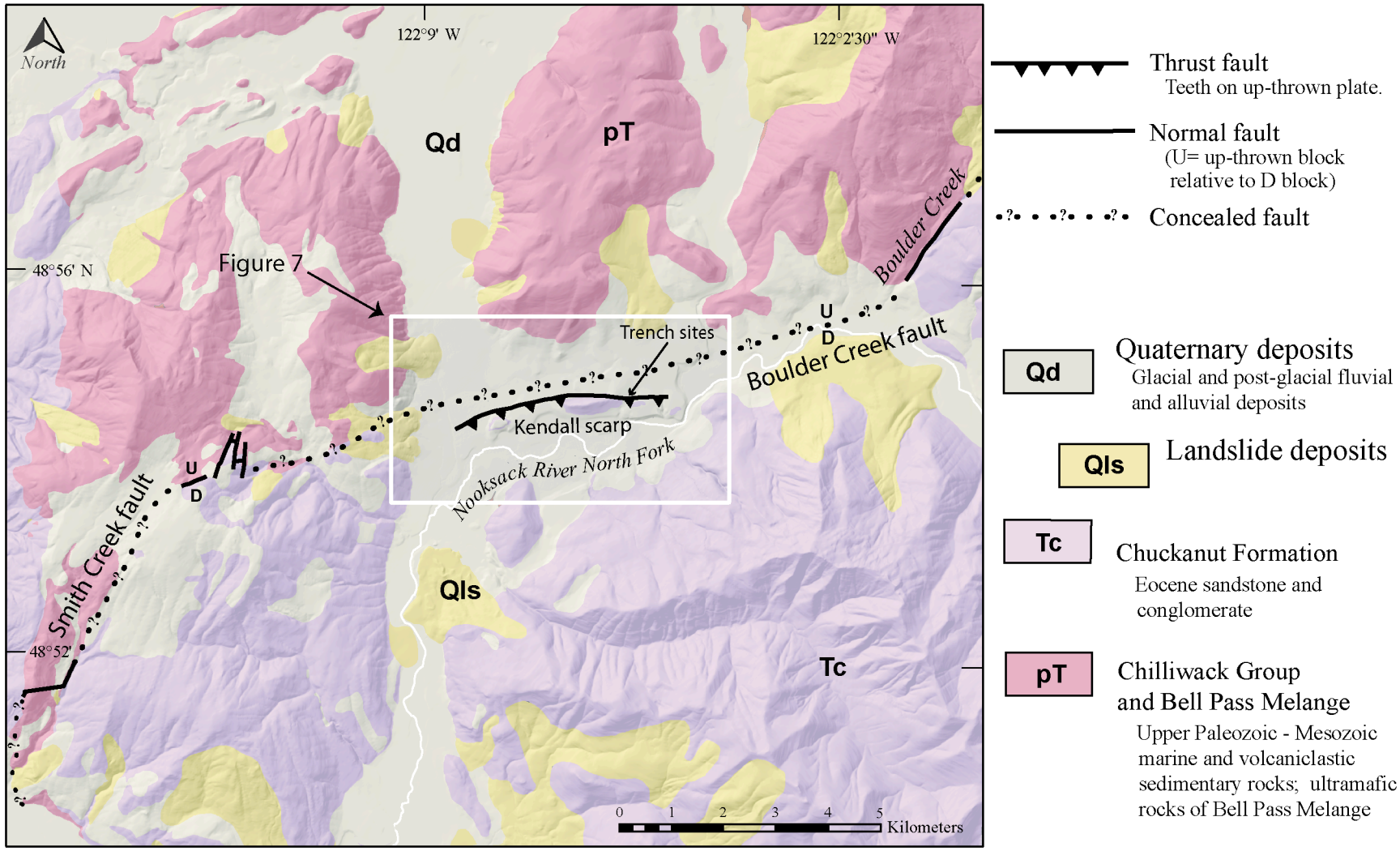

Figure 4: Generalized regional geology of the Kendall scarp area. Pre-Tertiary sedimentary and volcaniclastic rocks of the Chilliwack Group and Bell Pass Melange (pT) north of Boulder Creek fault are juxtaposed against Eocene Chuckanut Formation (Tc) sandstone and conglomerate south of Boulder Creek fault. Quaternary deposits (Qd) comprise both glacial and post-glacial deposits. Landslides (Qls) are post-glacial. Where fault is concealed by Quaternary sediments, placement of Boulder Creek fault is inferred by earlier workers. Map simplified from: Moen (1962), Mische (1966), Mische (1977), Brown et al. (1987), Kovanen (1996), Dragovich et al. (1997a), and Haugerud (written communication, 2006).

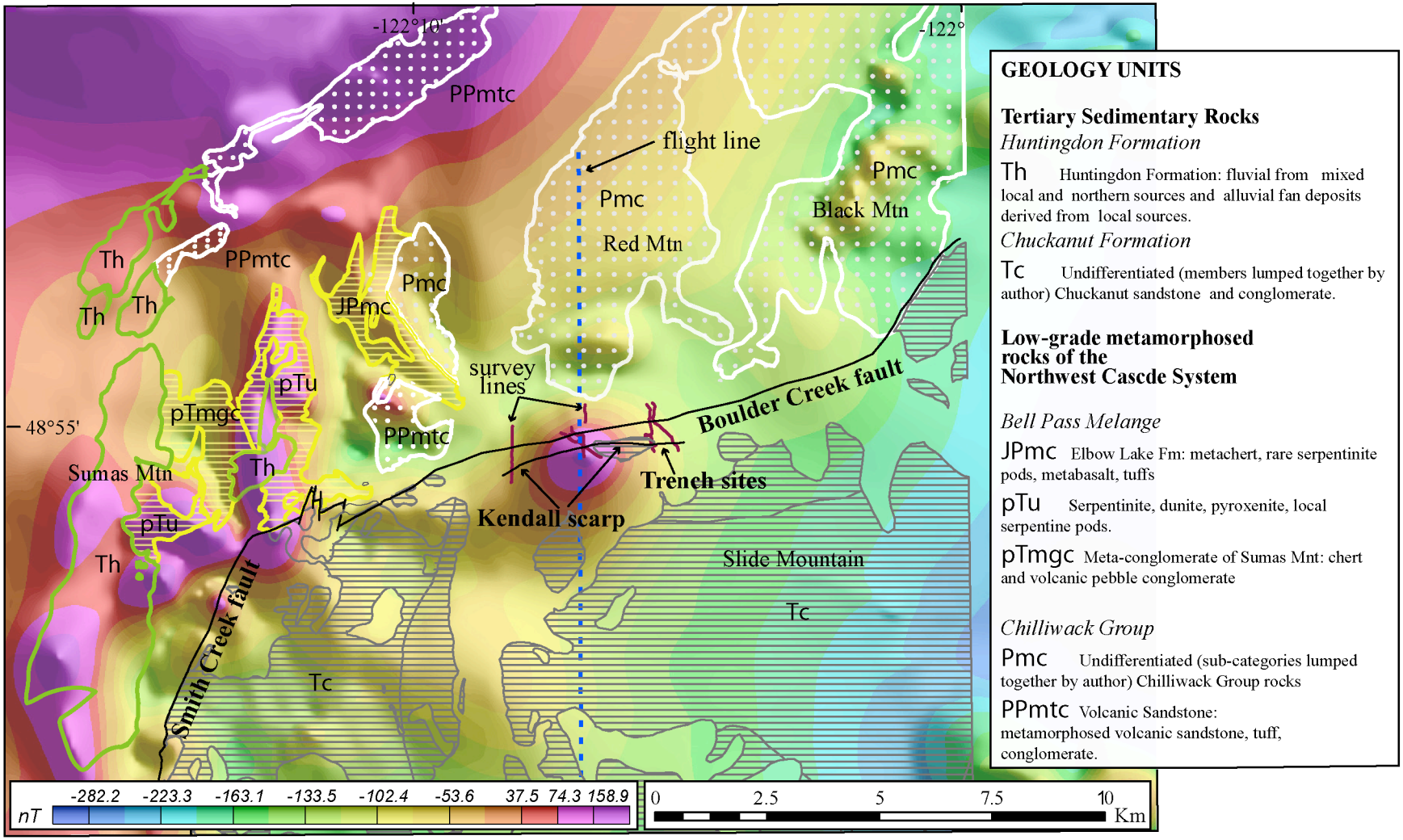

Figure 5: Aeromagnetic anomalies (Blakely et al., 1999) and generalized geology of Kendall-Maple Falls area. Anomaly measured in nT (nanotesla). Highlighted units are possible candidate sources of magnetic anomalies; yellow, Bell Pass Melange rocks; white, Chilliwack Group rocks; and lime green, Huntingdon Formation rocks. Sources of the magnetic anomaly closest to the Boulder Creek fault appear to be the Bell Pass Melange serpentinite and ultramafic rocks on Sumas Mountain and the Huntingdon Formation on the west side of Sumas Mountain. Geology sources: Johnson (1982), Dragovich et al. (1997a), Haugerud (2006, written communication.).

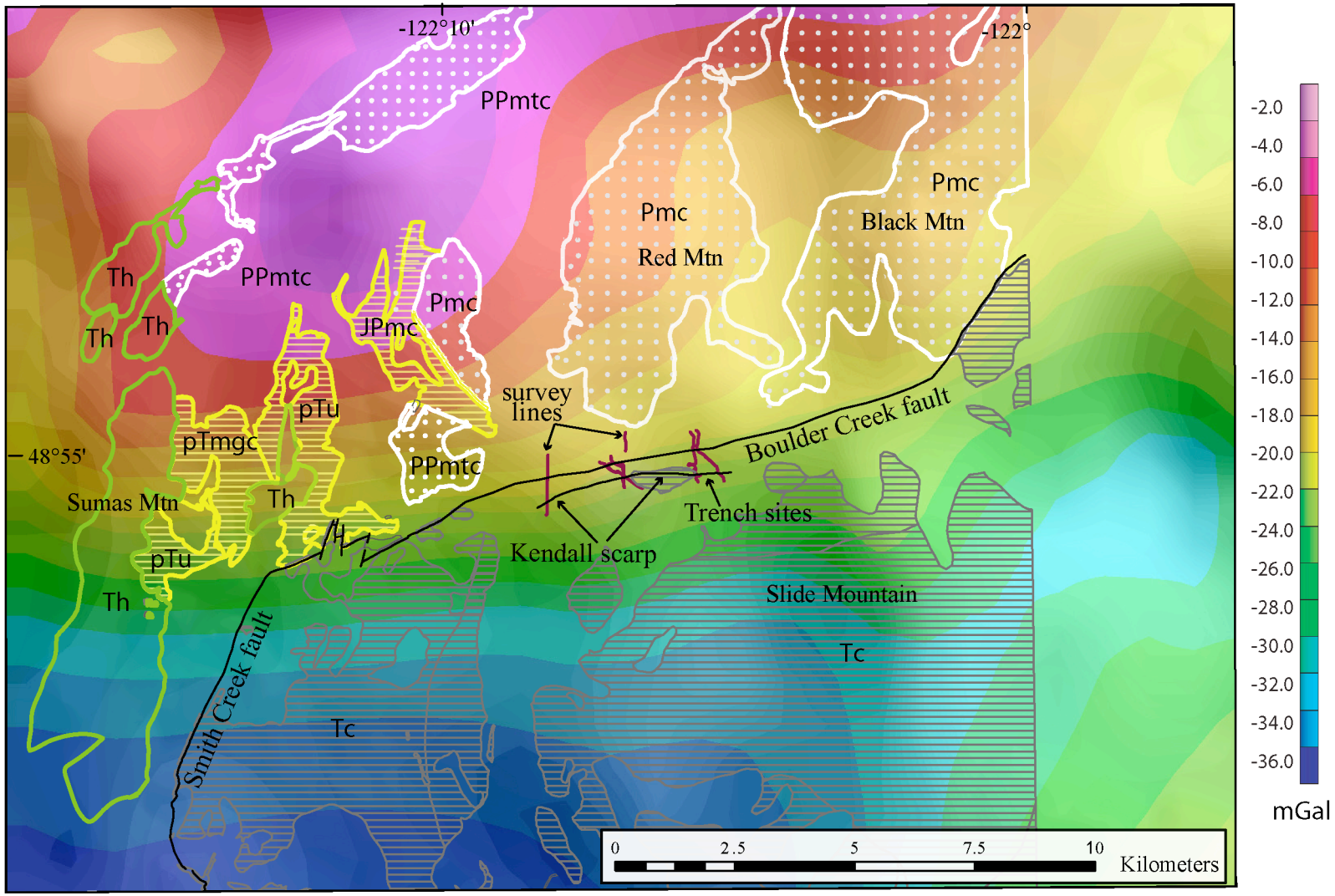

Figure 6: Isostatic Gravity map of area depicted in Figure 5. Source: Finn et al., 1991.

(PPmtc) in the northern margin of the study area (outlined in white in Fig. 5) (Johnson, 1982; Dragovich et al., 1997a).

The pattern of gravity data (Fig. 6) is similar to the trend of the magnetic data, with areas of greatest intensity north of the normal faults and areas of gravity lows south of the normal faults. However, the anomalous high magnetic intensities that mark the Kendall fault scarp, Bell Pass Melange rocks and Huntingdon Formation are not evident in the gravity data.

Post-Glacial Landscape

In the Kendall fault scarp area, evidence of glacial advance and retreat is plentiful (Fig. 7): broad outwash plains (Qow) of the Columbia and Nooksack valleys, valley walls lined by Vashon-age till (Qvt), glacial grooves scoured into bedrock visible in LiDAR images, and two moraines (Qsm) mapped by Kovanen (1996) and Kovanen and Easterbrook (2001). The thick blanket of outwash, offset and preserved in the Kendall fault scarp, was deposited during the Sumas stade, the last glacial advance in northwestern Washington (Armstrong et al., 1965). The Sumas stade occurred between 10,000 and 11,500 ^{14}C yr BP (Clague et al., 1997; Kovanen and Easterbrook, 2001). Kovanen (1996) and Kovanen and Easterbrook (2001) suggest that the last glaciers to inundate the valley emerged from the Mt. Baker – Mt. Shuksan area after the last Cordilleran ice sheet had receded after ~12,500 ^{14}C yr BP. A maximum age for the youngest outwash, derived from wood underlying glacial marine drift is 11,910 +/- 80 ^{14}C yr BP (Kovanen and Easterbrook, 2001). Charcoal extracted from within the outwash

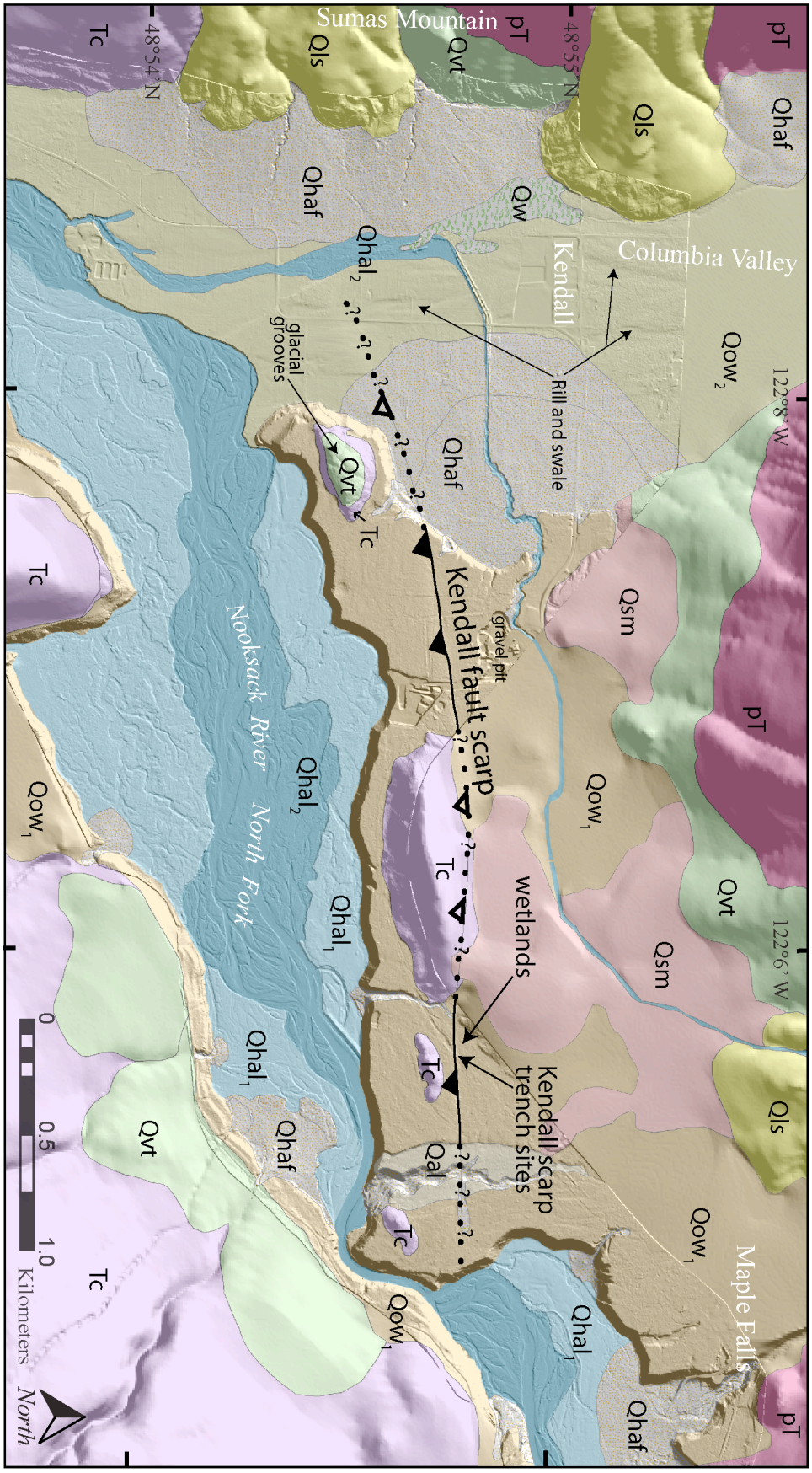

Figure 7: Surface geology map and map legend (following page) for Kendall scarp study site.

Map Symbol	Unit description of Quaternary deposits	Unit mapping and description data source
	Holocene deposits	
$Qhal_2$	Youngest (Holocene) alluvium; active stream channel	1
$Qhal_1$	Young (Holocene) alluvium; former active channel, now river terrace surfaces	1
Qls	Landslide deposits	2
Qw	Wetlands deposits	1
Qhaf	Holocene alluvial fan	2
Qal	Stream-related alluvium deposits of undetermined age; may be Late Pleistocene	3
	Sumas Stade deposits	
Qow_2	Youngest glaciofluvial outwash plain. Features N-S rills and swales	2
Qow_1	Glaciofluvial outwash plain; surface cut by Qow_2 outwash system	2
Qsm	End moraine (mapped as Kendall and Maple Falls moraines by Kovanen (1996, 2002))	4
	Vashon Stade deposits	
Qvt	Glacial till	5
	Pre-Quaternary rocks of the North Cascades	
Tc	Chuckanut Formation (Eocene) sandstone and conglomerate	6
pT	Chilliwack Group and Bell Pass Melange (Late Paleozoic - Mesozoic) deep marine sedimentary rocks, volcaniclastics, and ultramafics	7

1 Lidar/USGS 10m DEM, aerial photos, Haugerud (pers. comm.)
2 Lidar/USGS 10m DEM, aerial photos, Haugerud (pers. comm.), Kovanen 1996, Kovanen and others 2002
3 Lidar/USGS 10m DEM
4 Kovanen 1996, Kovanen and others 2002
5 Haugerud (pers. Comm. 2006), Dragovich, et al. 1997, Moen 1962, Lidar/USGS 10m DEM
6 Haugerud (pers. Comm. 2006), Dragovich, et al. 1997, Johnson 1982, Moen 1962, Lidar/USGS 10m DEM
7 Haugerud (pers. Comm. 2006), Dragovich, et al. 1997, Moen 1962, Lidar/USGS 10m DEM

Figure 7 continued

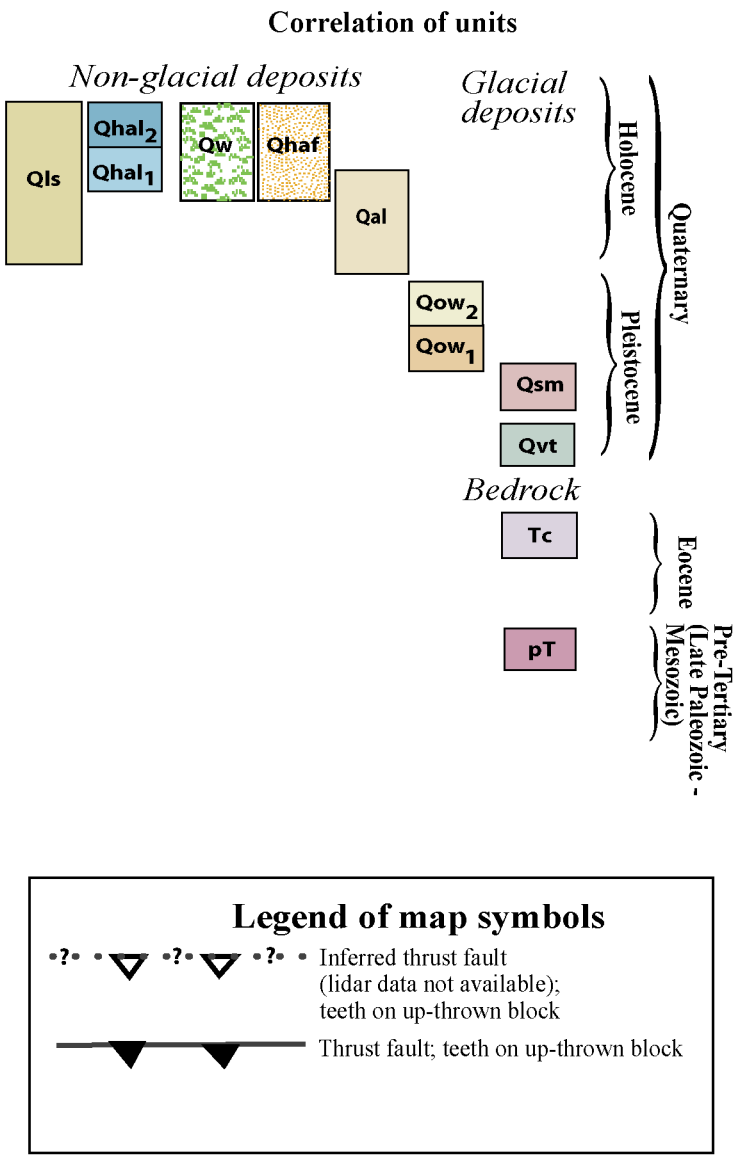

dates to 10,603 +/- 69 ^{14}C yr BP and 10,788 +/- 77 ^{14}C yr BP (Kovanen and Easterbrook, 2001).

Through aerial photograph and LiDAR image mapping, we delineate two outwash deposits, Qow_1 and Qow_2. The streams that deposited Qow_2 and imprinted rill and swale structures on the floor of the Columbia Valley, identified in LiDAR imaging, probably carved out the west-facing terrace riser that eroded Qow_1 (Fig. 7). Holocene-age deposits include fans (Qhaf) and landslides (Qls) that widely occur throughout the North Fork Valley (Figs. 4 and 7).

Extent of Kendall Fault Scarp

The Kendall fault scarp crosses the forested Qow_1 terrace about 500 m north of the Nooksack River (Fig. 8). It is visible in both aerial photos and LiDAR as a conspicuous 4.5 km linear feature along trend of the Boulder Creek fault (Fig. 4). The scarp is most prominent at the location of Stellar's Jay and Hornet trenches (Fig. 8) and becomes more diffuse to the west as it crosses from the Qow_1 terrace onto the Qow_2 plain (Figs. 7 and 8). Surface expression of the scarp eventually disappears to the west of Route 542 within the Columbia Valley alluvium east of a large alluvial fan emptying from Sumas Mountain (Fig. 7). The eastern edge of the scarp visible in LiDAR abruptly terminates at the edge of the terrace and active Nooksack channel.

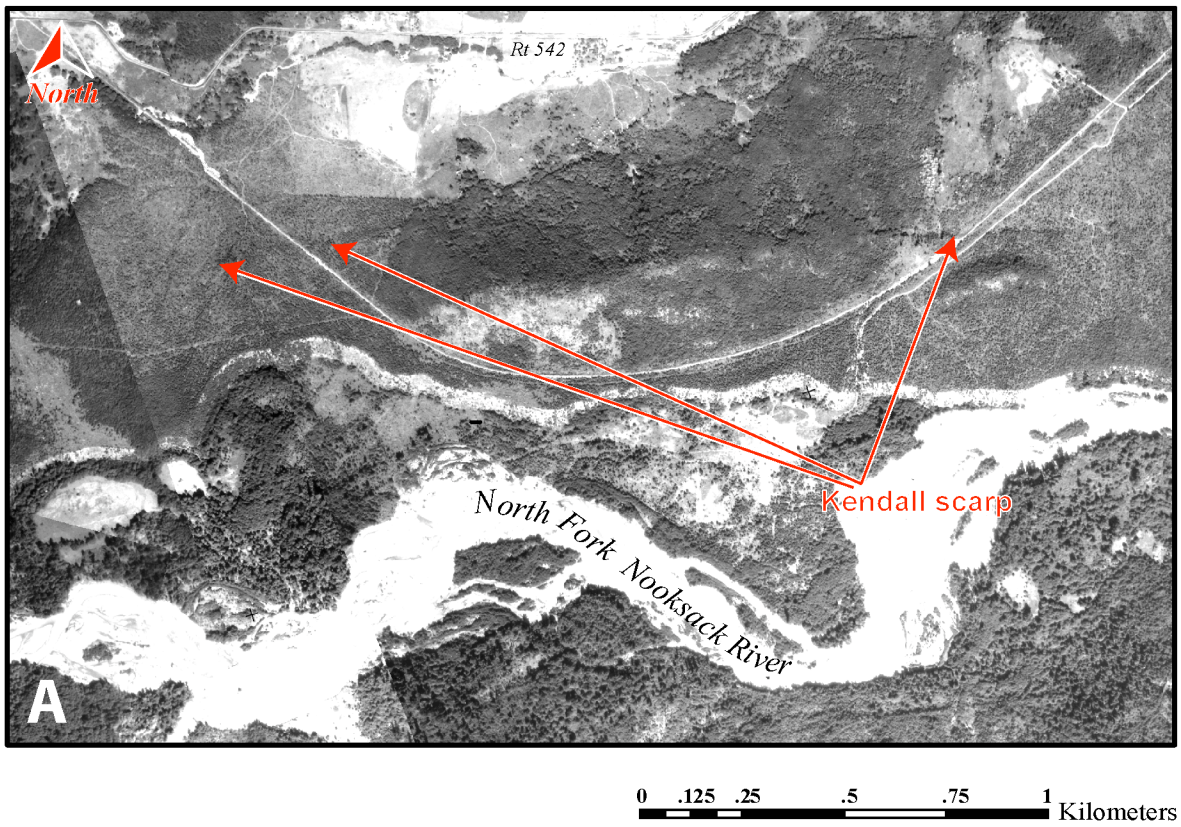
North
Rt 542
Kendall scarp
North Fork Nooksack River
A
0 .125 .25 .5 .75 1 Kilometers

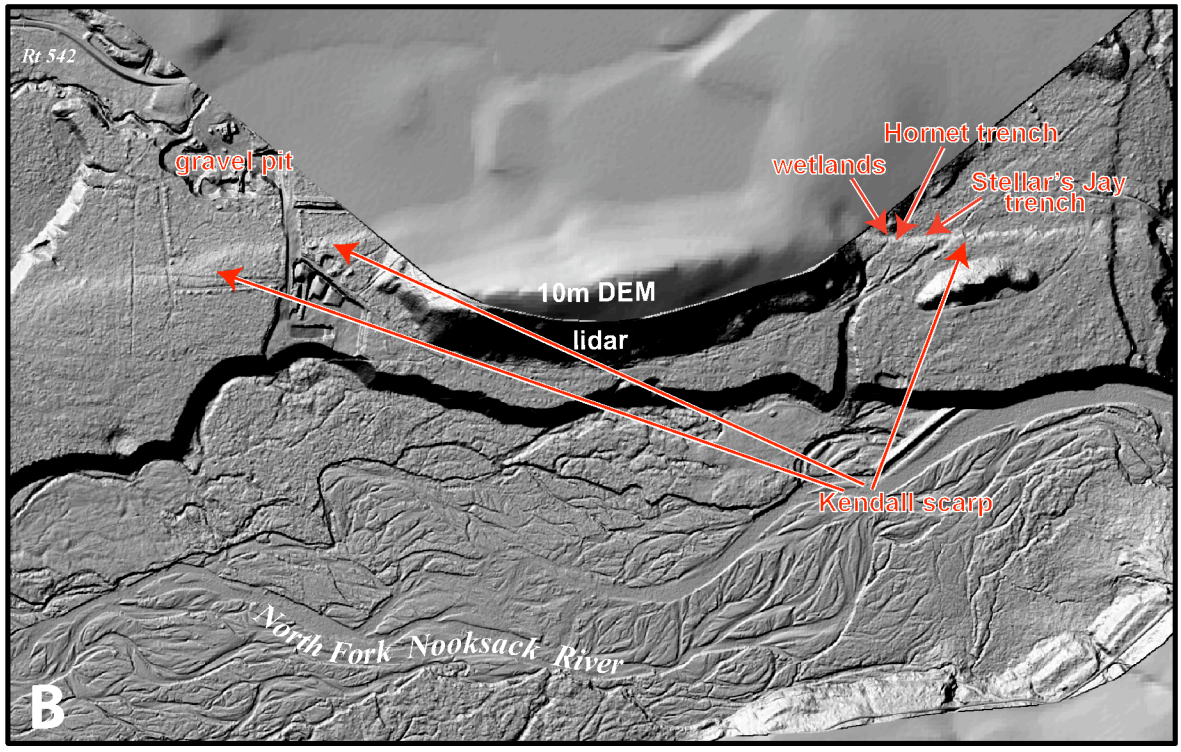
Rt 542
gravel pit
Hornet trench
wetlands
Stellar's Jay trench
10m DEM
lidar
Kendall scarp
North Fork Nooksack River
B

Figure 8

INVESTIGATIVE APPROACH AND METHODS

The Kendall scarp project is a collaborative effort. Although all project members were involved with most aspects of data collection in the trenches and wetland, primary responsibilities of the investigators are as follows: the author was responsible for Stellar's Jay trench investigtations, Brian Sherrod and Harvey Kelsey coordinated investigations in the Hornet trench, and Jonathan Hughes was responsible for the wetland investigations, with field assistance from Sherrod and the author. Richard Blakely provided the magnetic survey instruments and facilitated the ground survey. Puget Sound Lidar Consortium and Tim Hyatt with the Nooksack Tribe contributed the Nooksack River LiDAR data.

We excavated two trenches along the Kendall fault scarp segment that is most pronounced in LiDAR imaging (Figs. 7 and 8). Stellar's Jay and Hornet trenches were located 2 km southwest of Maple Falls and 4 km east of Kendall, approximately 500 m south of Route 542, and between an old railroad grade, the eastern edge of a 250 m high hill of Chuckanut sandstone, and The Glen Mobile Home Park (Fig. 8). Each trench was approximately 20 m long and had benched walls. We erected a 1m x 1m reference grid along the trench and mapped on Mylar-covered photo-mosaic images of the trench walls. Geological units are based on a unit code related to lithology, stratigraphic position, and inferred age (from oldest to youngest). Soil texture terms and organic material descriptions followed Natural Resources Conservation Service notation and

description (Schoeneberger et al., 2002). Primary color is the dominant Munsell color taken dry (moist color in parentheses).

In addition to trench excavations, we also recorded the stratigraphy of 20 cores from transects in the wetland that we infer was dammed by the fault scarp during earthquakes. The wetland location is about 10 m northwest of the Hornet trench location, on what we infer to be the fault footwall.

We investigated the deeper structures underlying the Boulder Creek fault by analyzing aeromagnetic data. The aeromagnetic data of the Kendall fault scarp are the products of a U.S. Geological Survey high-resolution aeromagnetic survey of the Puget Sound area (Blakely et al., 1999). The flight lines of the aeromagnetic survey were flown parallel and north-trending at an altitude of around 250 m with 400 m spacing. Base magnetometers provided corrections for time-varying magnetic fields. Total-field anomalies are the result of subtracting the International Geomagnetic Reference Field.

Increasing the anomaly imaging resolution required conducting a ground survey that mitigates the anomaly attenuation effects of flying a magnetometer above the ground surface. We conducted the ground survey using a cesium-vapor magnetometer backpack unit with real-time GPS navigation equipment. A base station magnetometer provided corrections for diurnal variations and external field fluctuations. Figures 5 shows the ground survey lines. The profile we analyzed came from a survey that crossed the scarp and Stellar's Jay trench site. All surveys were conducted at least 100-200 m from houses and roads in order to diminish the noise from roads, machinery and underground pipes.

To process the magnetic data and create models, we used GM-SYS and Oasis Montaj software to create 2-d geologic preliminary models from our magnetic data by forward modeling subsurface structures. By varying rock susceptibility parameters and magnetic body geometry, we created models of calculated value profiles that visually best fit the observed magnetic profiles for the aeromagnetic and ground survey. These parameters were based on geological knowledge of the field area, field measurements of rock susceptibility in the Kendall scarp area, and geometry parameters such as magnetic body shape and depth.

RESULTS

Stellar's Jay Trench

The Stellar's Jay trench excavation site was approximately 30 m east of Hornet trench and 40 m east of the wetland. The trench azimuth was perpendicular to the scarp, 353° N. The stratigraphy of Stellar's Jay trench consists of a thick sequence of sands and gravels overlain by paleo soils and faulting-related sandy gravels, all capped by a continuous modern soil. With the exception of the modern soil, all stratigraphic units are offset, disturbed, or caused by faulting.

Structure

The Stellar's Jay deformation zone is confined to 5 m of length in the trench starting at 8 m on the trench log (Figs. 9, 11 and Plate 1); whereas, trench stratigraphy outside of the deformation zone is undisturbed. The primary structural feature in Stellar's Jay trench is fault F1, which dips to the south between 25° in the lower trench to around 40° in its top 50 cm (Fig. 9). The fault is delineated by a well-defined zone of rotated clasts within the sand and gravel units of the lower trench and abrupt contacts between truncated and lithologically distinct units in the upper 1-2 m of the trench (Fig. 9). Fault F1 does not breach the modern soil. Fault F2 is located 60-80 cm above and parallel to F1 and forms the upper boundary of the rotated clast zone. Fault F2 becomes less distinct in the upper

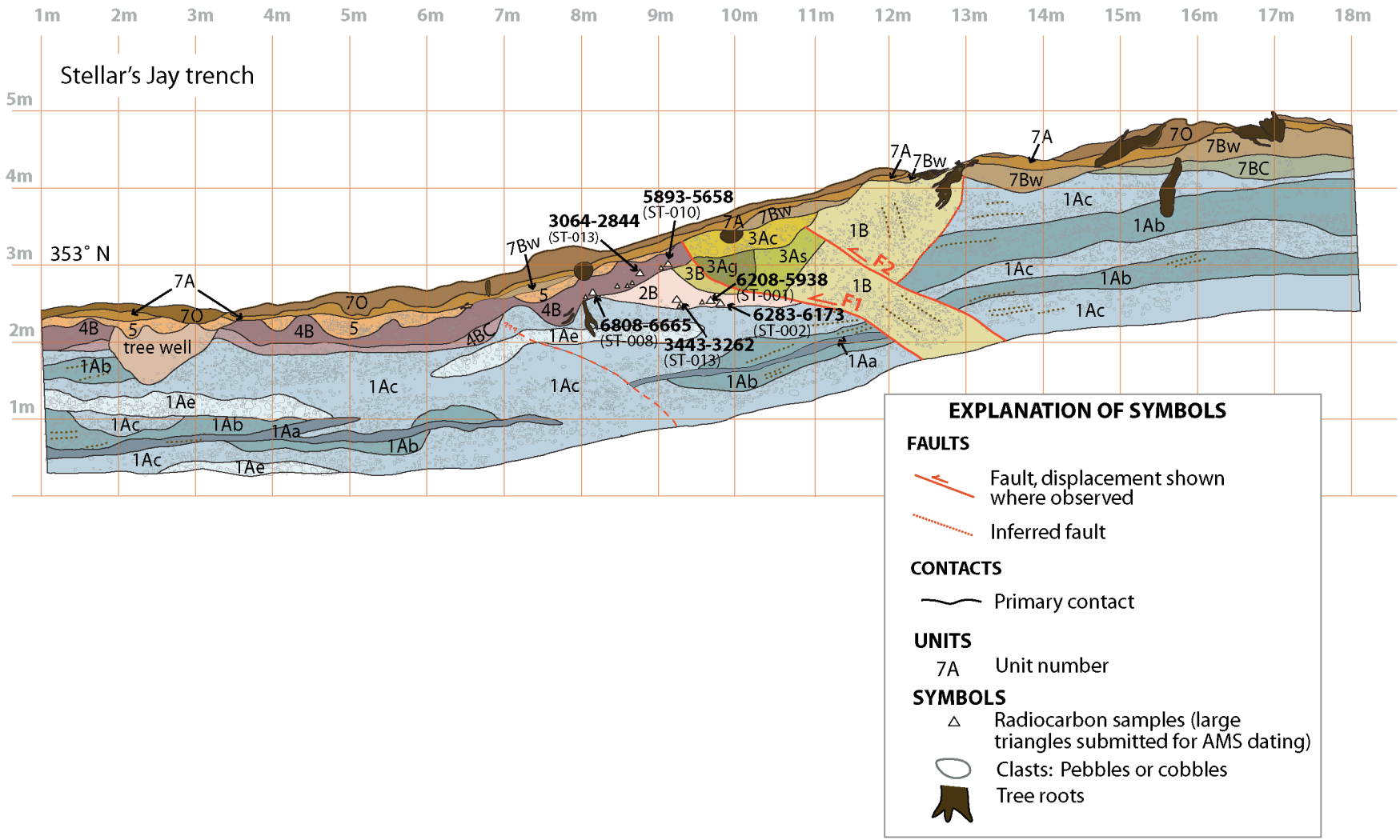

Figure 9: Stellar's Jay trench log.

UNIT	HORIZON	LITHOLOGY	MATRIX TEXTURE	COARSE FRACTION		MATRIX COLOR	ORGANIC MATERIAL	STRUCTURES	
				Pebbles	Cobbles			Depositional and/or soil structure	Tectonic Deformation
7O	O	Modern forest litter	Forest litter			10 YR 2/2	Leaves, woody fragments, and other organic detritus.	Surface soil organic horizon	None
7A	A	Sandy silt	Sandy clay loam	2-5%	<1%	5 YR 3/3	Roots:f 2 sh, m2 sh, c 1 sh	Surface soil, soil structure: 1 f sbk	None
7Bw	Bw	Sandy silt with pebbles	Sandy loam	5-10%	<2%	5 YR 4/4	Roots: 1 f sh; 2 m sh	Surface soil, soil structure: 1 f gr	None
7BC	BC	Sandy silt with pebbles	Sandy loam	10-20%	<1%	7.5 YR 4/4	Roots: 1 f sh; 2 m sh	Surface soil, soil structure: 1 f gr	None
5		Sandy silty gravel	Sandy loam	20-30%	10-15%	Varies	None	None	None
4B	buried B	Sandy silt	Sandy clay	0-20%	2%	10 YR 6/6	Roots: f 1 sv, m 2 sv, vc 1 v	Buried soil, soil structure: 1 f gr	Cut by F1
4BC	buried BC	Sandy silt with pebbles	Sandy loam	30%	5%	10 YR 6/6	Roots: f 1 sv, m 1 sv	Buried soil, soil structure: 1 f gr, disturbed by deep tree wells.	None
3B		Silty sand	Sandy loam	10%	<1%	10 YR 6/6	Roots: f 1 sv	None	Cut by F1
3Ac		Silty sandy gravel	Sandy loam	30%	5%	7.5 YR 4/4	Roots: 2 f sh, 1 m sh	None	Cut by F1 and possibly F2
3Ag		Silty sandy gravel	Sandy loam	30-40%	2%	10 YR 6/3	Roots: 2 f sh, 1 m sh	Weak sub-horizontal bedding of pebbles at base of unit	Cut and possibly rotated by F1
3As		Silty sand	Sandy loam	15-20%	None	2.5 Y 6/4	Roots: 1 f sh, 1 m sh	Weak sub-horizontal bedding at base of unit.	Cut and possibly rotated by F1
2B	buried B	Pebbly silt	Sandy clay loam	10-20%	None	10 YR 6/6	Roots: vf 1 sv, m 1sv, co 1sv	Buried soil, soil structure: 1 gr 1	Cut and plowed into wedge by F1
1B		Sandy gravel	Loamy sand	50%	5-10%	2.5 Y 6//4	Roots: 1 f sh, 1 m sh	Clast fabric is disrupted. Clasts between F1 and F2 are parallel to faults and rotated to vertical in hanging wall.	Cut, displaced, and clasts rotated by F1 and F2
1Aa		Sand	Loamy sand	10-20%	2%	2.5 Y 5/3	None	Planar and weak cross-bedding.	Cut and displaced by F1
1Ab		Pebbly sand	Sand	60%	2-5%	2.5 YR 5/3	None	Clasts imbricated in places; weak cross-bedding and planar beds within sandy pockets.	Cut and displaced by F1 and F2
1Ac		Sandy pebble-cobble	Sandy loam	60%	10%	2.5 Y 6/4	None	Clasts imbricated in places. Sand pockets have weak planar bedding.	Cut by F1 and F2
1Ae		Sand	Sand	40-50%	25-30%	2.5 Y 6/4	None	None	None

Figure 10: Log and unit description of Stellar's Jay trench. Unit designations are based on lithology, stratigraphic position, and inferred age. Texture, root terms, and soil horizon terms follow Natural Resources Conservation Service notation and description (Schoeneberger et al., 2002). Primary color is dominant Munsel color taken dry.

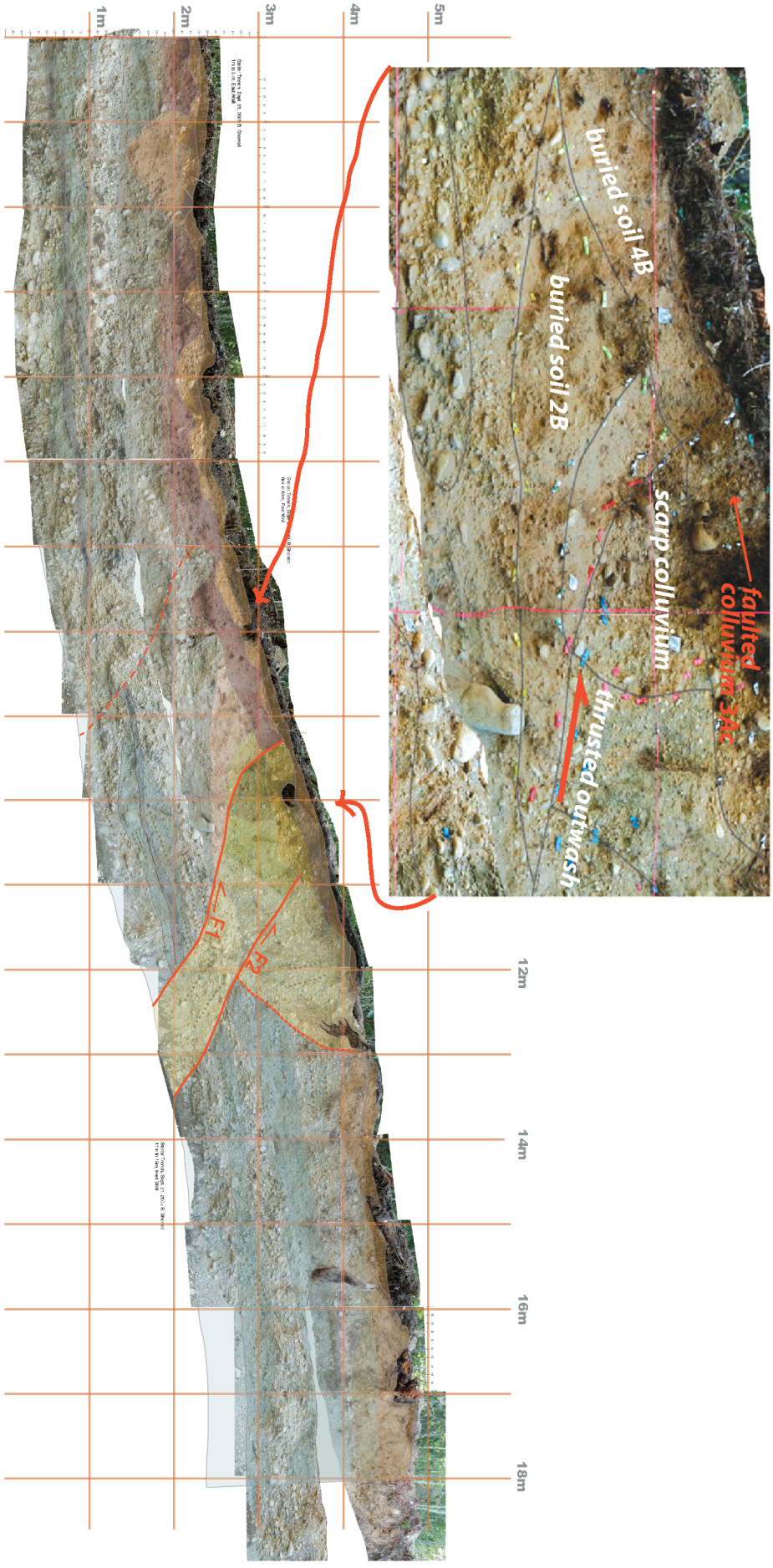

Figure 11: Photo-mosaic of Stellar's Jay trench with overlay of geology unit mapping from Figure 9 .

1.5 m of its extent. Gentle folding of the outwash deposits (1Aa-1Ae) is visible between 9 m and 18 m in the trench log (Fig. 9).

Stratigraphy

The lowest unit series found in Stellar's Jay trench, 1Aa through 1Ae, comprises discontinuous beds of sand and gravel that are distinguished by grain size (Figs. 9 and 10). Units 1Ab and 1Ac are thick (30cm - 2m), light yellowish brown, coarse, sandy gravel beds with intermingled, discontinuous and thinner sand beds (1Aa and 1Ae) (Fig. 9). Clasts are sub-rounded to sub-angular and range from pebble to cobble size. They make up 25-30% coarse fraction of 1Ae. The sand beds (1Aa and 1Ab) exhibit weak to moderate sub-horizontal planar-bedding and cross-bedding. The units with predominantly pebble-size clasts (1Ab and 1Ac) show weak to moderate imbrication (Figs. 9 and 10). Based on lithology, stratigraphic position beneath the modern soil, and prior mapping (Kovanen and Easterbrook, 2001), we infer that these units are Late Pleistocene outwash.

Unit 1B is stratally disturbed outwash deposit divided by fault F2 into two sections (Figs. 9, 11 and Plate 1). The lower section is a rectangular body bounded by faults F1 and F2. It contains clasts sheared and rotated parallel to the faults; moreover, the clast fabric delineates faults F1 and F2 in the lower trench. The upper section has a clast fabric with moderate sub-vertical orientation. This wedge of 1B overlies fault F2 and disappears beneath the modern soil and unit 3Ac. The tilted orientation of the clast fabric and jumbled appearance distinguishes the wedge from adjacent 1A units that do not appear to be disturbed by faulting. The contact zone between units 1A and 1B ranges

between 10-20 cm in thickness. Based on the distinct fabric of rotated and sheared clasts within 1B and its close proximity to the faults, we infer the entire unit 1B was disturbed and displaced by faulting along F1 and F2.

Unit 2B is a brownish yellow, silty clay loam that overlies the outwash deposits (Figs. 9,10, 11 and Plate 1). It is separated from the underlying outwash deposits by a clear contact and distinct matrix material transition from sand in the outwash to silt-clay above the contact. Soil structure, i.e., ped formation, is weak granular and pebbles make up about 10-20% of the coarse fraction. Unit 2B is located only below Fault F1. Based on the presence of soil structure, lithology (Fig. 10), and stratigraphic position directly above the outwash deposit and below fault F1, we infer that 2B is the lowest buried soil truncated by fault F1.

Unit 3B is a 1 m long sliver of brownish yellow, silty sand between 2B and fault F1 (Fig. 9 and 10). Unit 3As is a fault-bounded, light yellowish-brown pocket of silty sand that contains 15-20% pebbles and is weakly bedded at its base. Unit 3As is separated from overlying 1B by fault F2. This contact is somewhat diffuse but is defined by a difference in both matrix material and pebble content, with a sand matrix in 1B and a silt-clay matrix in 3As. Pebble content also distinguishes 3As from 3Ag: the pebble content of 3Ag is 30-40% compared to 15-20% pebbles in 3As. Similar to 3As, 3Ag is weakly bedded at the base. Both 3Ag and 3As overlie 3B and the buried soil, 2B. Unit 3Ac, a 20 cm thick lens of brown silty sandy gravel, caps both 3Ag and 3As (Figs. 9 and 10). Soil structure is not present in 3B, 3Ag, 3As, or 3Ac. Due to the lack of soil structure, the silty, sandy, and pebbly lithologies (Fig. 10), and stratigraphic position as

discrete fault-bounded wedges that overlie a buried soil (2B), we interpret these units to be scarp colluvium deposited during or after earthquakes.

Overlying the outwash deposits (1Aa through 1Ae) and lower buried soil 2B, 4B is a 20-30 cm thick continuous bed of brownish yellow, sandy clay with weak, fine granular soil structure and contains, at most, 20% pebbles (Figs. 9 and 10). Unit 4B terminates abruptly against fault F1 and fault colluvium, 3Ac (Fig.11 and Plate 1 for photo showing contact). Soil texture differences and a higher level of consolidation distinguishes 4B from underlying buried soil 2B (Fig. 10). Unit 4B is interpreted to be the upper buried soil in the trench, and this is based on 4B soil structure and its fault contact with colluvium 3Ac (Fig.11 and Plate 1). Beginning 1.5 m north of the contact with 2B, 4B is underlain by a thin (~10 cm) discontinuous bed of 4BC, a pebbly sandy silt containing 30% pebbles. A silty matrix, less oxidized grain content, and lower pebble content in 4BC distinguishes it from the underlying sandy outwash deposits. Similar to 4B, 4BC shows a weak, fine granular soil structure and is interpreted to be the BC-horizon of the upper buried soil.

Buried soil, 4B, is overlain by discontinuous pockets of unit 5 (Figs. 9 and10, Plate 1), which is lighter in color, and less consolidated than both 4B and the modern soil (unit 7). Unit 5 has a higher pebble and cobble fraction than unit 4B, and exhibits no soil structure. Due to this lack of soil structure, high pebble and cobble content, and its location in the footwall at the base of fault F1 and above 4B, we consider unit 5 to be scarp colluvium.

The modern soil (unit 7) caps all buried soil, colluvuim units, and faults in the trench (Fig. 9). The texture of the Bw and BC horizons (7Bw and 7BC) is sandy loam and the soil structure for both B-horizons is weak granular (Fig. 10). The pebble content and Munsell color value increases in the lower horizons. Only a small sliver of 7Bw exists in the footwall, and 7BC is absent. The A and O horizons (units 7A and 7O) are horizontally continuous throughout the trench. Unit 7A is a sandy clay with less than 5% pebbles and has a weak sub-angular blocky soil structure. Unit 7O consists of unconsolidated forest litter.

Evidence for Holocene Earthquakes

All units within Stellar's Jay trench are offset and deformed by faulting except for the surface soil (unit 7) and the upper-most colluvium (unit 5) (Fig 9). Based on the trench exposures we have evidence for at least three earthquakes. The first earthquake did not rupture the surface but folded the outwash deposits (1Aa-1Ae). The current scarp height of 2.5 m exceeds the vertical component of offset for the oldest soil faulted during the oldest ground-rupturing earthquake, 1.7 m. Thus, the height of the fold scarp probably was ~80 cm (Table 1). Uncertainties in the height of the fold scarp after the first earthquake come from two sources: uncertainty in measuring the modern scarp height and uncertainty in measuring the minimum vertical separation of the oldest buried soil from the trench log.

Table 1: Trench deformation

Trench	A. Structural relief of top of unit 1 (m)	B. Vertical component of offset of oldest buried soil	C. Inferred relief of fold scarp caused by first earthquake (m) (A minus B)
Stellar's Jay	2.5	1.7	0.8
Hornet	1.9	0.5	1.4

The second earthquake (event 2) ruptured the ground surface along faults F1 and F2. Faulting along F1 thrust glacial outwash (1Aa-1Ae) over the oldest buried soil (unit 2B). The vertical displacement is a minimum of 80 cm, but the maximum vertical displacement is unknown because 2B is eroded from the hanging wall. Fault F2 probably moved concurrently with F1 during the second earthquake because F2 does not appear to cut through colluvial unit 3Ac. The motion of F2 relative to F1 rotated the clast fabric of the outwash parallel to the faults. Unit 1B above the fault tip of F2 was fractured and rotated such that the once horizontal clasts became vertical. As a result of the earthquake, colluvium 3B was deposited directly below the scarp on the footwall above soil 2B. Soil 4B then developed on the surface.

The third and most recent earthquake ruptured along fault F1 and faulted colluvium from the second earthquake (unit 3Ac) against truncated buried soil 4B (Figs. 9,11 and Plate 1). Colluvium from the third earthquake (unit 5) was eroded from the scarp face and deposited on the footwall slope. A possible fault, only weakly visible within the outwash sand and gravel, is located between 7 m and 9 m in the trench log (dashed red line, Fig. 9). The pebble fabric near this fault is weakly disrupted with some clasts rotated parallel to the proposed fault, and unit 1Aa appears to be abruptly cut off. The timing of motion on this structure, if it is a fault, with respect to faults F1 and F2 cannot be determined because no offset of beds can be determined.

Hornet Trench

Similar to Stellar's Jay trench, Hornet trench stratigraphy comprises a thick sequence of sand and gravel overlain by buried soils and faulting-related silty gravel, all capped by a horizontally continuous modern soil. All units are either disturbed or generated by faulting, except the modern soils.

Structure

The primary fault in Hornet trench, fault F1, dips 35°-40° to the south and terminates beneath the modern soil at 3.3 m height in the trench log (Fig. 12). The location of fault F1 can be inferred by a plane of rotated clasts and offset beds. A smaller fault, F2, branches from fault F1 at 2.6 m height in the trench log (Fig. 12) and ends at approximately the same height as fault F1. Three other faults (F3, F4, F5) are located between 8 m and 10 m in the trench exposure (Fig. 12). They dip to the south more steeply than fault F1, around 45°. Sand and gravel beds in the lower trench between faults F1 and F3 are rotated and dip between 30° and 40°. Smaller faults or fractures branch from fault F4 and zones of rotated clasts define the location of these faults.

Stratigraphy

The lowest stratigraphic units of Hornet trench are sand and gravel beds (1Aa-1Ae), interpreted to be glacial outwash using the same criteria as in Stellar's Jay trench (Fig. 12).

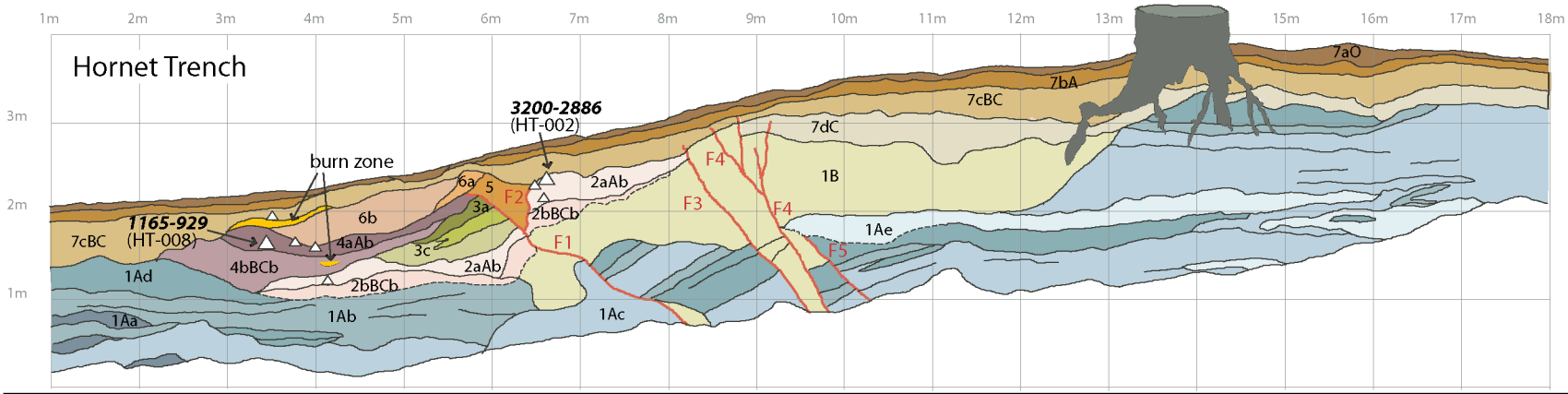

UNIT	HORIZON	LITHOLOGY	MATRIX TEXTURE	COARSE FRACTION		MATRIX COLOR	ORGANIC MATERIAL	STRUCTURES	
				Pebbles	Cobbles			Depositional and/or Soil Structures	Tectonic Deformation
7aO	O	Plant remains	(Forest litter)			10YR2/2 (10YR2/1)	None	None	None
7bA	A	Sandy silt to silty sand	Silt loam to loam	<1%		10YR4/3 (10YR2/2)	Roots – 2-3, f, sv-h; 3, vf, sv-h	Soil structure – 2, m, sbk	None
7cBC	BC	Sandy silt to silty	Silt loam to loam	2-5%		10YR4/3 (7.5YR2.5/2)	Roots – 1-2, vf-f, sv-h	Soil structure – 2, m, sbk	None
7dC	C	Cobbly pebbly sand	Sand	30-40%	<2%	10R5/4	Roots – 1, f, sv	Massive	Cut by F4
6b	--	Sandy silt to silty sand	Silt loam to loam	<2%		10YR5/4	Roots – 1, f, h	Soil structure – 1-2, vf-f, sbk	None
6a	--	Pebbly silty sand	Silt loam to loam	~15%		2.5Y5/4	Roots – 1, co, h; 2-3, vf-f, h	Soil structure – 1-2, vf-f, sbk	None
5	--	Pebbly sand	Sand	15-25%		2.5Y5/4	Roots – 1, co, h; 1, m, h; 3, vf-f, sv	Soil structure – 1-2, m, sbk	Possibly rotated by movement on F1 and F2
4aAb	A_b	Pebbly sandy silt	Silt loam to loam	<1%		10YR5/4 (10YR3/4	Roots – 1-2, vf-f, sv-h	Soil structure – 2-3, vf-m, sbk	Cut by F1 and possibly folded by F1
4bBCb	BC_b	Pebbly sandy silt	Silt loam to loam	~2%		10YR5/4 (10YR3/4)	Roots – 1, f-m, h	Soil structure – 1-2, vf-m, gr-sbk	Cut by F1 and possibly folded by F1
3a	--	Cobbly pebbly sand	Sand	20-30%	~1%	2.5Y5/3	Roots – 1-2, vf-f, sv	Massive	Cut by F1 and possibly folded by F1
3b	--	Fine to coarse sand	Sand	<1%		2.5Y5/3	Roots – 1, f-m, h	Planar, graded bedding	Cut by F1 and possibly folded by F1
3c	--	Pebbly sand	Sand	~15-20%		10YR5/4	Roots – 1-2, f-vf, sh-v	Massive	Cut by F1 and possibly folded by F1
2aAb	A_b	Sandy silt	Silt loam to loam	5-10%		10YR4/3 (10YR3/2)	Roots – 1, f, sh	Soil structure – 3, m-f, sbk	Cut and folded by movement on F1
2bBCb	BC_b	Pebbly sand	Loamy sand	~20%		10YR5/3	Roots – 1, f, sv	None	Cut and folded by movement on F1
1B	--	Cobbly pebbly sand	Sand	30-40%	<2%	2.5Y5/3	Roots – 1, f, sv	Massive	Stratally disrupted and cut by F1 – F5
1Ae	--	Cobbly sand	Sand (v. fine to coarse)	30-40%	~10%	2.5Y6/4	Roots – 1, f, sv-v	Imbrication of pebbles and cobbles in places	Cut by F3 and F4
1Ad	--	Pebbly sand	Sand (fine to coarse)	60-70%		2.5Y5/3	Roots – 1, co, sv;	Low angle cross beds or planar beds	Folded and faulted. Steeply dipping to north (25°-35°),cut by F1, F3, and F5
1Ac	--	Cobbly pebbly sand	Sand	30-40%	<2%	2.5Y4/3	Roots – 1, f-m, sh	Massive	Cut by movement on F1, F4, and F5
1Ab	--	Pebbly coarse sand	Sand	30-40%		10YR4/3	None	Low angle cross beds or planar beds	Stratally disrupted and diplaced by faulting along F1, F3, F4, and F5
1Aa	--	Coarse sand with granules, pebbles	Sand	<1%		2.5Y4/3	None	Massive	None

Figure 12 (preceding page): Log and unit description of Hornet trench. Unit designations are based on lithology, stratigraphic position, and inferred age. Texture, root terms, and soil horizon terms follow Natural Resources Conservation Service notation and description (Schoeneberger et al., 2002). Primary color is dominant Munsel color taken dry.

Some sandy beds show occasional planar and low angle cross-bedding (1Ad and 1Ab), and pebbles and cobbles in 1Ae are imbricated in places (Fig. 12). Similar to Stellar's Jay trench, 1B consists of outwash deposits that are stratally disrupted by and located proximate to the faults.

Unit 2aAb is a dark yellowish-brown silt loam to loam with moderate sub-angular blocky soil structure (Fig. 12). This unit comprises two elongate bodies separated by fault F1. Based on the presence of soil structure (ped formation), lithology (Fig. 12), and stratigraphic position directly above the outwash deposit, we infer that 2aAb is the lowest buried soil A-horizon offset by fault F1. The underlying BC-horizon (2bBCb) is a brown loamy sand with moderate sub-angular blocky soil structure and contains about 10% more pebbles than 2bBCb. 2bBCb is offset by fault F1 and appears above it.

Units 3a, 3b, and 3c form a wedge located above buried soil 2aAb and only below fault F1. Unit 3 consists of cobbly-pebbly sand with graded and planar bedding in places and no soil structure. Because the wedge of 3a, 3b, and 3c is located above buried soil 2aAb and directly below fault F1, has a sandy, cobbly lithology and does not show soil structure, we infer unit 3 is scarp colluvium.

Units 4aAb and 4bBCb consist of yellowish-brown, silt loam to loam above scarp colluvium unit 3. Both exhibit soil structure, but 4bBCb has a weaker sub-angular blocky soil structure than overlying 4aAb. Units 4aAb and 4bBCb are buried Ab and BCb horizons, based on their lithology, soil structure and stratigraphic position above scarp colluvium, unit 3, and adjacent to fault F1. This upper buried soil (unit 4) is only

found below fault F1 whereas the lower buried soil (unit 2) is found above fault F1, as well.

Directly overlying the upper buried soil is another wedge of pebbly sand, unit 5, which is located between the tip of the fault F1 and fault F2 (Fig. 12). Units 6a and 6b are lenses of pebbly silty sand and sandy silt that overlie unit 5 and the upper buried soil. Fault F1 does not cut units 6a and 6b. We interpret units 5, 6a and 6b to be colluvium based on their stratigraphic position above the upper buried soil, 4aAb, and adjacent to faults F1 and F2.

Modern soils (7-series), including a bright pink burn lens, cover the glacial outwash, buried soils, and colluvium deposits. Faults of the Hornet trench disappear beneath the modern soils, and thus, do not displace them.

Evidence for Holocene Earthquakes

The first earthquake recorded in the trench (event 1) did not rupture the ground surface but produced a gentle fold scarp. The modern scarp height, 1.9 m, exceeds the vertical of offset for the oldest buried soil, 0.5 m, and thus the fold scarp relief is ~1.4 m (Table 1 and Fig.12). During the second earthquake (event 2), fault F1 offset the outwash and soil unit 2. Faulting disturbed the clast fabric of unit 1 producing 1B. Colluvium deposits (3c, 3a, 3b) raveled down the scarp face onto the footwall and piled on top of the former ground surface, burying the soil to form buried soil unit 2. Soil (unit 4) formed on the slope below the fault scarp.

During the third and most recent earthquake (event 3), fault F1 truncated both colluvial deposits of unit 3 and overlying upper buried soil (4bBCb and 4aAb). Probably concurrently, the fault tip collapsed and another small fault (F2) branched off causing clasts caught between F1 and F2 to shear and rotate. This wedge of colluvium (unit 5), consisting of colluvium from the second event, was thrust over buried soil 4aAb. Following this earthquake, sediment eroded from the scarp face and collected at the base of the scarp on the footwall as lenses of colluvium, 6a and 6b. Surface soil (soil unit 7) developed on the footwall and hangingwall surface after the last event.

Kendall Wetland

Stratigraphy

The stratigraphy of a wetland can record hydrological changes that accompany ground deformation after an earthquake. The core stratigraphy of the Kendall wetland consists of interlayered aquatic and forest deposits: gyttja, an organic-rich deposit that accumulates in standing water, and a detrital peat that composes the forest soils. Core stratigraphy showed three sequences of these deposits.

The lowest deposits in the wetland core stratigraphy are inorganic stream-deposited glacially reworked sandy deposits (Fig. 13) (Hughes, written communication, 2006). The glacially reworked sediment consists of dark, greenish gray loam, sandy loam, and sand that together are more than 1 m thick in some locations. The upper-most sandy

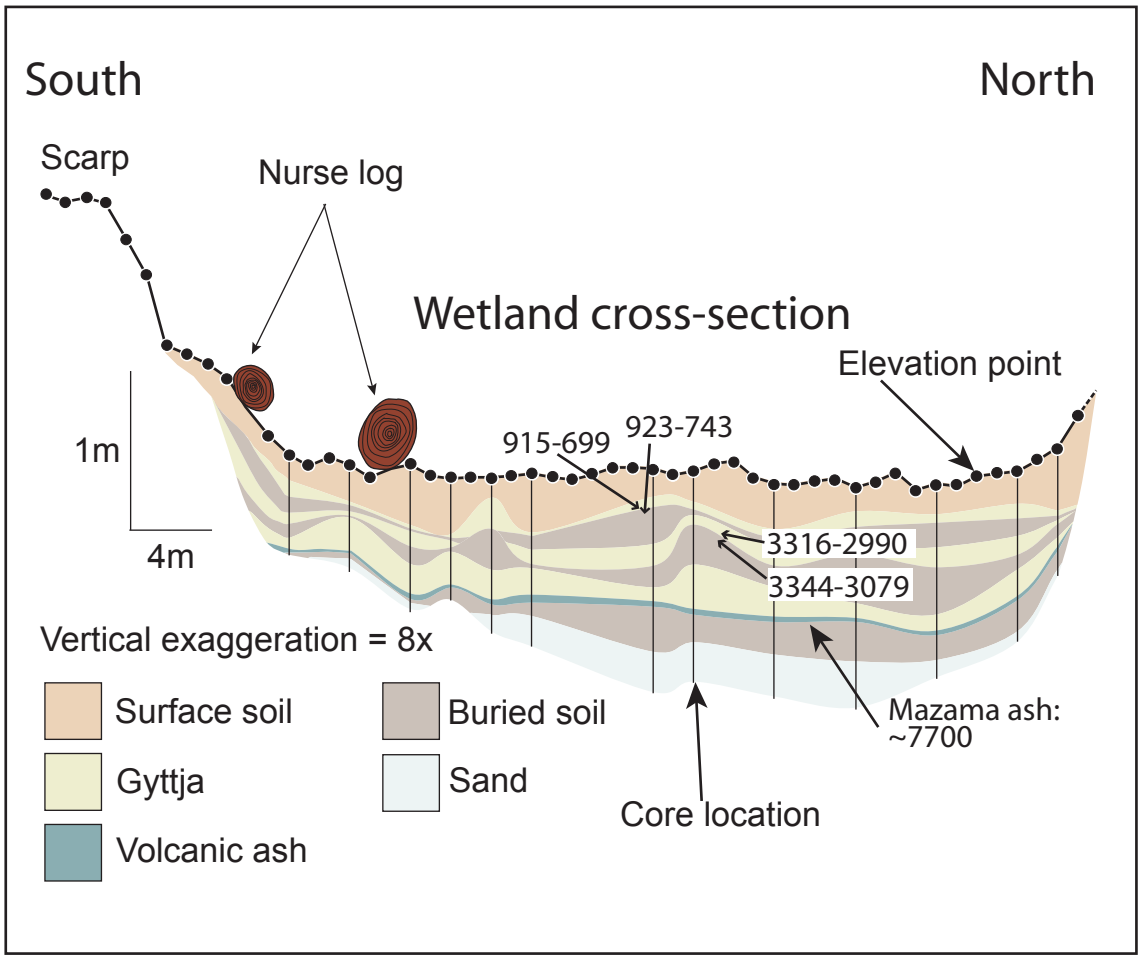

Figure 13: Cross section of wetland adjacent to Kendall scarp. Ages (yrs BP) are for the buried soils (Table 2). Wetland stratigraphy collected by Jonathan Hughes, unpublished data. Figure modified from Sherrod et al., unpublished data.

glacial deposit is overlain by the lowest organic peaty soil, a dark-gray to black (Munsell color designation) silt loam, which can be more than 30-cm thick in places. The organic content increases up-sequence to form the detrital peat. This lowest soil is overlain by a light beige gyttja deposit that contains at its base a distinctive yellowish-brown Mazama volcanic ash (~7700 yr BP) that is about 2-cm thick (identified using electron microprobe analysis; Foit, written communication, 2006).

Above the lowest gyttja, two more sequences of detrital peat are abruptly overlain by gyttja (Fig. 13) (Hughes, written communication, 2006). The detrital peat can contain fossil *Tsuga heterophylla* (western hemlock) needles, *Thuja plicata* (western red cedar) scales, *Spiraea douglasii* (hardhack) fruits, *Rubus sp.* (salmonberry) seeds, herbaceous roots, wood fragments and charcoal. The bark-rich contact that distinguishes the detrital peat from overlying gyttja includes *Polygonum sp*. (knotweed) and *Scirpus microcarpus* (sedge) seeds. The gyttja is typically dark-gray to very dark-brown and ranges from 4- to 20-cm thick. Common components include wood, charcoal, and pebbles. Organic content decreases up-sequence as gyttja transitions to a 20 to 40 cm thick, very dark-brown to black silt loam detrital peat (2- to 40-cm thick) (Hughes, written communication, 2006).

Evidence for Earthquakes

Based on stratigraphic sequences of gyttja and forest soil, we infer that the wetland records three earthquakes. The earliest earthquake recorded in the wetland occurred when the Kendall fault scarp dammed a small stream flowing south toward the

Nooksack River and resulted in development of the wetland. When the site converted to the wetland, gyttja was deposited on forest soil. As the wetland gradually dried, possibly after the south-flowing streams found another outlet or eroded through the scarp, forest soil again developed on the site. The scarp height increased during two subsequent earthquakes, and each time the site responded by deposition of gyttja on forest soil.

Ages of Buried Soils at Trench and Wetland Sites

In order to determine the earthquake timing, we collected detrital charcoal for radiocarbon dating from buried soils in both trenches and wetland cores (Table 2). Detrital charcoal samples from the trenches provide a maximum limiting age for an earthquake event because it is possible that older charcoal can be recycled into a younger deposit. Furthermore, the age of the charcoal may pre-date the age of the soil horizon by several hundred years, depending on the age of the burned tree, or charcoal source (Gavin, 2001). Plant material samples from the wetland core samples may provide more reliable dates because, compared to charcoal, the dated plant material found in the cores was deposited and buried *in situ* and thus was less susceptible to erosion and reworking.

Buried soils in the trenches and wetland yield mid-to-late Holocene maximum limiting ages (Table 2). In the wetland, the upper buried soil is 915-699 yrs BP, based on

Table 2: Radiocarbon ages, Kendall fault scarp

Sample I.D.	Lab I.D.	^{14}C age BP*	Calibrated years BP σ-2 ∅	Dated material description
Kendall fault scarp wetland				
KST3-22-22	210789	880 +/- 40	915-699	Plant material from gyttja above upper soil contact
KST3-22-29	210790	920 +/- 40	923-743	Plant material from gyttja above upper soil contact
KM-FG 53-55 Split A	223978	3020 +/- 40	3344-3079	*Thuja plicata* leaves and conifer needles from above middle soil contact
KM-FG 55-57 Split A	223979	2960 +/- 40	3316-2990	*Thuja plicata* leaves and conifer needles from top of middle soil
Hornet trench				
HT-008	210083	1100 +/- 40	1165-929	Charcoal from upper buried soil
HT-002	210084	2890 +/- 40	3200-2886	Charcoal from lower buried soil
Stellar's Jay trench				
ST-008	216885	5930 +/- 40	6878-6665	Charcoal from upper buried soil
ST-013	216886	2820 +/- 40	3064-2803	Charcoal from upper buried soil
ST-010	220069	5020 +/- 40	5893-5658	Charcoal from upper buried soil
ST-001	216883	5300 +/- 50	6258-5938	Charcoal from lower buried soil
ST-002	216884	5380 +/- 40	6283-6008	Charcoal from lower buried soil
ST-012	220070	3130 +/- 40	3443-3262	Charcoal from lower buried soil

*All samples processed at Beta Analytic, Inc.
∅Calibrations using CALIB 5.0 (Stuiver and Reimer, 1993; Stuiver et al., 2005)

plant material sampled directly above the buried soil, and 923-743 yrs BP for plant material within the upper buried soil (Fig. 13) (Hughes, written communication, 2006). Detrital charcoal from the upper buried soil (4aAb) of Hornet trench is 1165-929 yrs BP (Fig. 12) (Sherrod, written communication, 2006). Ages for the plant material in the middle buried soil of the wetland are 3344-3070 and 3316-2990 yrs BP (Fig. 12) (Hughes, written communication, 2006). Detrital charcoal from the lower buried soil (2aAb) in Hornet trench is 3200-2886 yrs BP (Fig. 12) (Sherrod, written communication, 2006). Six detrital charcoal samples yielded dates for the Stellar's Jay trench. Radiocarbon ages from the upper buried soil are: 6878-6665 yrs BP, 5893-5658 yrs BP, and 3064-2803 yrs BP. The lower buried soil dates are: 6258-5938 yrs BP, 6283-6008 yrs BP, and 2442-3262 yrs BP (Table 2 and Fig. 9).

Magnetic Anomaly Study

Aeromagnetic and Ground Survey Data

The Kendall aeromagnetic anomaly is a distinct ~10 km^2 oval-shaped magnetic high that straddles the Kendall scarp and Boulder Creek fault less than ~300 m from the trench sites (Fig. 5). We selected aeromagnetic data from a flight line that bisected the center of anomaly, ~500 m west of the trench sites (Fig. 5). The anomaly peak is sharp and the profile is steepest on the north limb (Figs. 14A and 14B). From peak to trough the anomaly intensity varies from about 180 nT to -150 nT (nanotesla is a unit of measure of

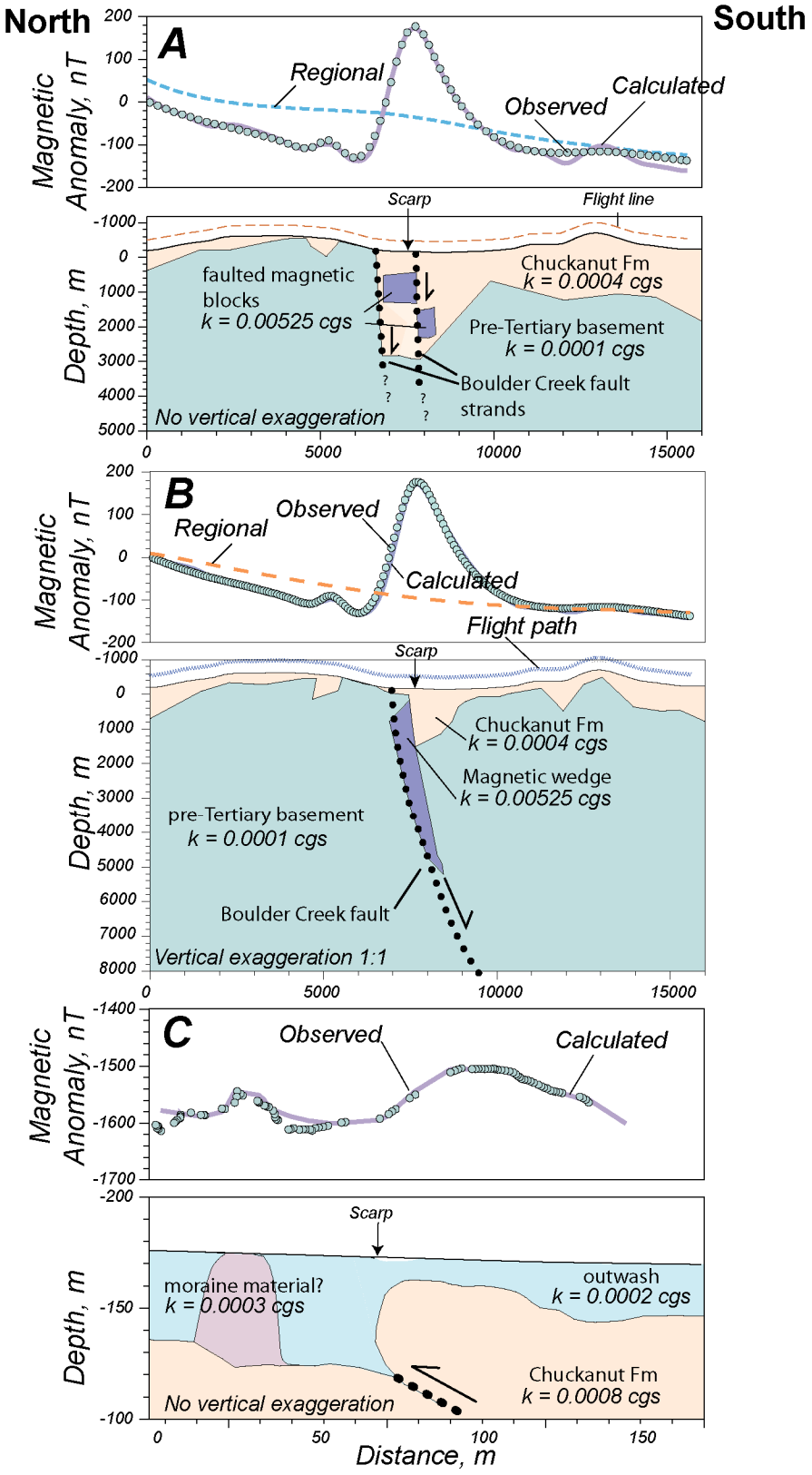

Figure 14: Aeromagnetic anomaly model of the Boulder Creek fault. Magnetic susceptibility (K) in cgs units. Upper box, observed (green dots) and calculated (purple line) magnetic profile. Lower box, calculated model. Boulder Creek fault is black dashed line. A.Two-block faulted serpentinite conglomerate within Chuckanut basin. B. Alternative aeromagnetic anomaly model of the Boulder Creek fault: sliver of serpentinite caught in the Boulder Creek fault. C. Ground Survey magnetic model of the Kendall scarp fault.

the magnetic flux density) (Figs. 5, 14A, and 14B). The north side tail increases steadily about 100 nT north from the anomaly peak. We used a graphical approach to find the anomaly depth, Peter's Method described by Blakely (1995). This method is based on the principle that the anomaly slope steepness depends on the depth of the magnetic body. The depth to the top of the Kendall anomaly is approximately 600-800 meters, which agrees with the models described below (Fig. 14).

The ground survey profile (Fig. 14C) that crosses the scarp at the Stellar's Jay trench site (Fig. 5) resulted in an anomaly with a broad peak and a leading edge that coincides with the trench location (Fig. 14C). The data are somewhat patchy due to noise from buried pipes encountered while conducting the ground survey; obvious noise-related peaks were removed from the data set.

Boulder Creek Fault - Kendall Fault Scarp Magnetic Anomaly Models

We constructed simple models of the observed magnetic anomaly that crosses the Boulder Creek fault and Kendall fault scarp in an attempt to explain the following: how rock type and faulting along the Boulder Creek fault can account for the observed magnetic data (Figs. 5 and 14), and whether magnetic data could help resolve any structural connection between the Boulder Creek fault and the Kendall fault scarp.

In order to construct the models, we set a model parameter, magnetic susceptibility, based on the susceptibility of field measurements and known rock types of the area. For the primary magnetic body, we used a serpentinite magnetic susceptibility $5x10^{-3}$ cgs (cm-gm-s system of susceptibility measurement) (Saad, 1969) to constrain

material susceptibilities in our models. We chose serpentinite as the material that most affects the regional magnetic signature and anomaly source because it is a local rock type (Sumas Mountain pTu, Fig. 5) that is highly magnetic with a potentially low density depending on degree of serpentinization. Consequently, serpentine rocks can have a strong magnetic expression and a weak gravity signature (Finn et al., 1991), which is consistent with geophysical observations near the Kendall fault scarp: both the Kendall anomaly and the serpentine-bearing pTu pods bear strong magnetic signals that are absent from the gravity data (Figs. 5 and 6). However, gravity station spacing was sparse in places and thus, gravity signals may be muted because of potentially poor data quality.

We collected susceptibility measurements from local rock outcrops of Chuckanut rocks, pre-Tertiary Chilliwack rocks, and glacial outwash in a gravel pit near the trench sites to estimate the susceptibility values in the models (Fig. 14A-C). We sampled only the Maple Falls Member of the Chuckanut that forms the hill adjacent to the trench sites (Fig. 7) and contains a high percentage of greenstone clasts compared to other Chuckanut Formation members (Johnson, 1982). Therefore, these rocks may be slightly more magnetic on average than the formation as a whole. These values ranged from $4x10^{-4}$ (cgs) to $8x10^{-4}$ (cgs). Susceptibility measurements of glacial outwash in the gravel pit (Fig. 7) are generally around $2x10^{-4}$ (cgs). A regional magnetic field included in the model (Figs. 14A and 14B) reflects observed long-wavelength magnetic fields possibly produced by the strongly magnetic rocks farther north or deeper in the crust (dark purple areas, Fig. 5).

We generated two simple models using the aeromagnetic data to explain the Boulder Creek fault-Kendall fault scarp anomaly as a product of highly magnetic material located at 600-800 m depth below the Boulder Creek fault (Figs. 14A and 14B). Due to the pronounced, narrow curve of the observed data, both models suggest a steeply dipping or near vertical magnetic body (Figs. 14A and 14B). Additionally, since the curve is steepest on the north limb we infer that two possible models of the magnetic body are either two faulted bodies with the down-dropped block to the south (Fig. 14A), or a single body that dips slightly to the south (Fig. 14B). The two-block version models a wedge of serpentine-rich conglomerate faulted during or after being deposited within the Maple Falls Member of the Chuckanut as the basin formed along the Boulder Creek fault (Fig. 14A). In the second model, a sliver of local pre-Tertiary serpentine is caught in the fault zone, possibly during basin formation (Fig. 14B). The models were most sensitive to changes in the serpentine body and much less so to the surrounding pre-Tertiary and Chuckanut rocks. Consequently, surrounding rock geometries in the models are relatively schematic.

Given our data constraints, we are not able to determine which model is more accurate or eliminate alternative models that might not involve faulting. We might be able to better define the fault location and geometry with more and better data constraints to add to the magnetic models. These parameters could include seismic or bore hole data, or improved bedrock mapping.

The survey line used in the ground survey model (Fig. 14C) represents the best quality data of our ground surveys. Even though some data points are removed from the observed profile, a low-amplitude rise remains in the profile (Fig. 14C). One model of the profile is

a north-verging uplift of slightly more magnetic Chuckanut rocks approaching the surface within a less magnetic outwash deposit (Fig. 14C). Another model could be the uplift of deeper outwash deposits that contain rocks with a higher susceptibility than the outwash measured in the gravel pit. The slight rise in the observed magnetic data north of the scarp anomaly peak may be explained by a moraine deposit or debris from the adjacent Chuckanut rock hill that contains slightly more magnetic clasts than the surrounding outwash. As with the aeromagnetic models, our constraints are minimal and could be refined with additional parameters. In this case shallow seismic data could be very useful to image at depth the fault recorded in the Kendall trenches.

DISCUSSION

Earthquake History of the Kendall Fault Scarp

The timing of the most recent earthquake, 1165-699 yr BP, is constrained by radiocarbon ages from the upper buried soil in the wetland and in the Hornet trench. Plant material at the upper contact of the upper buried soil in the wetland core dates to between 923-699 yrs BP (Fig. 13 and Table 2). This age range is slightly younger than the age of the detrital charcoal in the upper buried soil (4aAb) of the Hornet trench, with a maximum-limiting age of 1165-929 yrs BP (Fig. 12 and Table 2). Detrital charcoal from the upper buried soils (4B) of the Stellar's Jay trench provides no age information due to probable recycling of older charcoal within the upper buried soil (Fig. 9 and Table 2).

Detrital charcoal from the lower buried soil (2aAb) in Hornet trench provides an age of 3200-2886 yrs BP for the penultimate earthquake (Fig. 12 and Table 2). This is the oldest surface rupture earthquake recorded in the trenches. The age of penultimate earthquake is indicated by plant material found in the middle buried soil of the wetland, which dates to 3344-3079 and 3316-2990 yrs BP (Fig. 13 and Table 2). In the Stellar's Jay trench we can infer that the penultimate earthquake post-dates the youngest detrital charcoal sample, 3443-3262 yrs BP, which is slightly older than the detrital charcoal age for the Hornet trench second earthquake (Fig. 9 and Table 2).

Mazama ash provides a single age constraint for the oldest earthquake recorded by the folding at the trench sites and by initial ponding at the wetland site. Since the ash is located above the oldest buried soil found in the wetland cores and within the lower

part of the oldest gyttja, the folding and first wetland flood occurred shortly before the ~7700 yr BP deposition of the Mazama ash (Fig. 13).

Retrodeformation of the Stellar's Jay Trench

Retrodeformation of the Stellar's Jay trench log (Fig. 15) shows a schematic representation of deformation caused by three earthquakes and the stratigraphic evolution of the Kendall fault scarp during its growth. After the end of glacial outwash deposition, the outwash terrace surface stabilized to form soil (2B) (Fig. 15a). Shortly before 7700 yr BP, northward compression and faulting was recorded as folding (event 1) of outwash and existing soil, 2B (Fig. 15b).

During the second earthquake (event 2), around 3000 yr BP, outwash was thrust northward burying soil 2B along faults F1 and F2 (Fig. 15c). As a result of the second earthquake, the tip of fault F2 was deformed and splayed (red dashed line) causing rotation to near vertical of outwash gravel (Fig. 15d). Sand and gravel bedding between faults F1 and F2 was sheared and clasts rotated parallel to the fault plane between F1 and F2 (unit 1B). During and shortly after the second earthquake, sand and gravel raveled down the scarp face and collected in small fans at the base of the scarp and on the footwall (unit 3, Fig. 15d). The white dashed line shows an idealized erosion surface formed as the scarp degraded and colluvium was transported across the scarp (Fig. 15d). Soil 4B eventually developed on the scarp and ground surface (Fig. 15e).

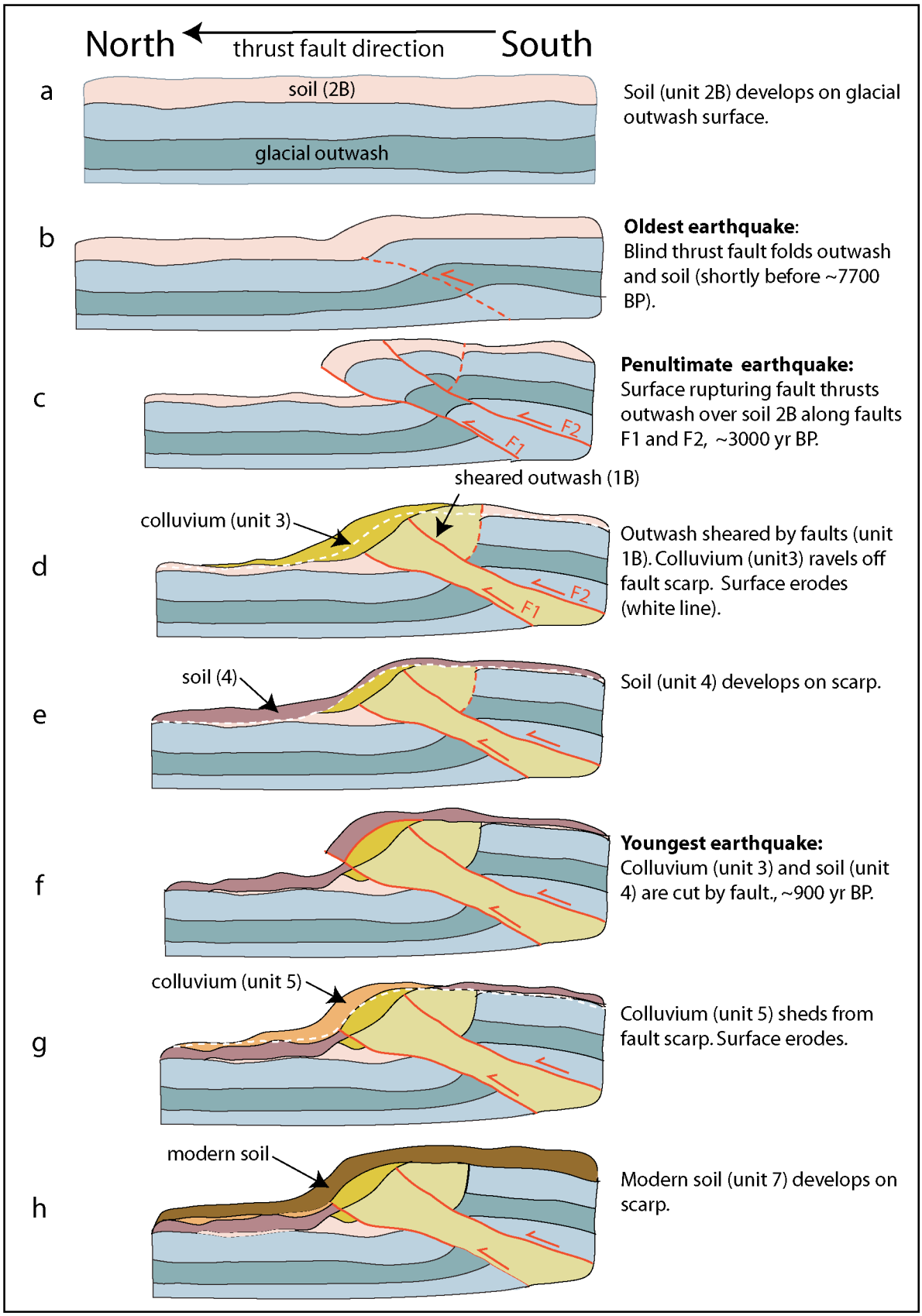

Figure 15: Retro-deformation of the Kendall scarp. Units pictured are simplified from unit classes in Fig. 9.

The third and most recent earthquake occurred around 900 yr BP and thrust colluvium (unit 3) over soil 4B along fault F1 (Fig. 15f). Truncated and orphaned event 2 colluvium (unit 3; 3B in Fig. 9) was sandwiched between F1 and soil 2B within the footwall (Fig. 15f). During and after the most recent earthquake, the fault tip collapsed and colluvium, unit 5, covered the scarp surface, footwall, and existing soil 4B (Figure 15g). Unit 5 is only visible in the footwall because fault colluvium probably was eroded from the lower part of the hanging wall after faulting. The white line in Fig. 15g represents the erosion surface formed as the new scarp degraded. The modern soil (unit 7) developed over the scarp surface (Fig. 15h).

The deformation sequence in the Hornet trench, not presented in a figure here, is similar to that for the Stellar's Jay trench. Shortly before ~7700 yr BP, glacial outwash and surface soil were folded. Next, glacial outwash (1Aa-1Ae) thrust over lower soils (2bBCb and 2aAb) along fault F1 during the first surface rupturing earthquake (~3000 yr BP) (Fig. 12). This resulted in deposition of fault colluvium and debris (3c, 3b, 3a) that covered the ground surface. Then, the most recent earthquake (~1000 yr BP) faulted outwash and buried a second soil, (4bBcb and 4aAb) with colluvium (5, 6a, 6b) along the same fault. Finally, modern soil horizons (unit 7) developed at the ground surface (Fig. 12).

Evaluation of the Magnetic Anomaly

The aeromagnetic anomaly models do not provide adequate constraints on the Boulder Creek fault geometry, slip direction or location. Considering the anomaly is oval

in shape rather than linear, probably it does not represent the magnetic contrast between two fault-juxtaposed materials along a fault trace. The anomaly, however, may indirectly locate the fault trace by identifying the strong magnetic expression of a wedge or wedges of highly magnetic material caught within the fault zone. Although the models did not constrain the fault geometry, they illustrate that the shape of the magnetic body or bodies can vary, but the body probably is highly magnetic, vertically elongated, and steeply dipping (Fig. 14A and 14B). The aeromagnetic models also do not confirm or refute reverse slip, documented in the trench data. Although the ground survey data hint at north-verging uplift in the location of the fault scarp, they do not resolve the relationship between the Kendall fault scarp and a deeper structure, the Boulder Creek fault. Ultimately, a seismic study may be better suited to image the shape of the magnetic body, contrain the fault location and geometry, and clarify the structural link between the the Boulder Creek fault and the Kendall fault scarp.

Kendall Fault Scarp Within the Context of Recent Seismicity

The Deming area, 10 km southwest of the Kendall fault scarp, has experienced several M 4.0 or greater earthquakes since 1969 (Pacific Northwest Seismic Network, 2006) (Figs. 3, 16). The 1990 Deming shallow earthquake swarm produced one of the largest earthquakes (M 5.0) to occur in the northern Puget Sound between 1920 and 1990, as well as several M 4.0 aftershocks (Pacific Northwest Seismic Network, 2006; Dragovich et al., 1997b). In 1990, a temporary seismic network installed near the epicenter recorded approximately 1800 earthquakes, most earthquakes occurring within 3.0 km of the surface (Dragovich et al., 1997b).

Dragovich et al. (1997b) suggest the seismicity may be a result of northward thrusting of Chuckanut Formation over pre-Tertiary Mount Josephine semischist along a thin-skinned decollement, the Macaulay Creek fault (Fig. 16). The fault is 2-3 km west of the location of the shallow earthquakes. The thrust motion of Macaulay Creek fault (Fig. 16) may be taken up by the re-activated Boulder Creek fault and left-lateral slip along the Smith Creek fault. Alternatively, all three faults may be one composite thrust fault that wraps around the Chuckanut basin and daylights as a fault scarp or scarps along the Boulder Creek fault (Dragovich, written communication, 2006). A structural and active tectonic link between the three faults is tenuous and the only surface rupture structure yet located in the area is the Kendall fault scarp.

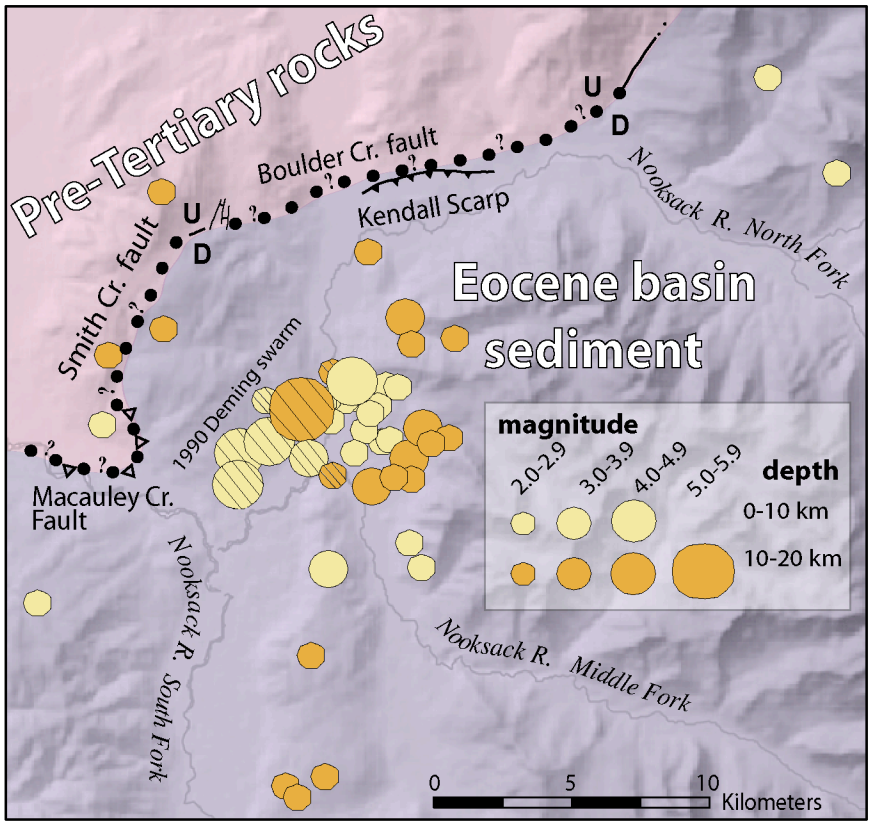

Figure 16: Schematic tectonic map showing possible linkage of existing faults that may accommodate late Quaternary northward vergence of Eocene basin sediments (Chuckanut Fm.) over Pre-Tertiary rocks (after Dragovich, et al., 1997b). Earthquake epicenters since 1969 from Pacific Northwest Seismic Network catalog.

Future Work

Close spatial proximity between the Boulder Creek fault and the Kendall fault scarp suggests it is likely that the fault scarp is the result of recent reverse motion along a fault strand within a Boulder Creek fault zone. However, more studies are necessary to link the two conclusively. For example, seismic reflection surveys might be able to image the deeper structures below the fault scarp and constrain subsurface fault geometry and location. Likewise, the magnetic models presented in this study could be improved by adding parameters such as borehole or well data and seismic data. Moreover, continued geological fieldwork may provide evidence of fault scarps along the mapped trace of the Boulder Creek fault where it is not covered by glacial sediment.

LiDAR imaging has been a great asset for identifying fault scarps in the Puget Sound region (Haugerud, et al., 2003), and this study is no exception. Obtaining more LiDAR data for Whatcom County is critical to locating surface deformation features beneath the dense vegetation of Western Washington. However, aerial photos from post-logging may also be useful. Although the Kendall fault scarp was initially identified on LiDAR imaging and not aerial photos, the fault scarp is clearly visible on the 1933 aerial photo shown in Figure 8A. In this same photo, another linear feature located about 500 m north of the Kendall fault scarp is visible (Figs. 8 and 17). Field-checking this feature would be one way to test whether the Kendall fault scarp is a solitary feature or one of several active strands that may compose the Boulder Creek fault.

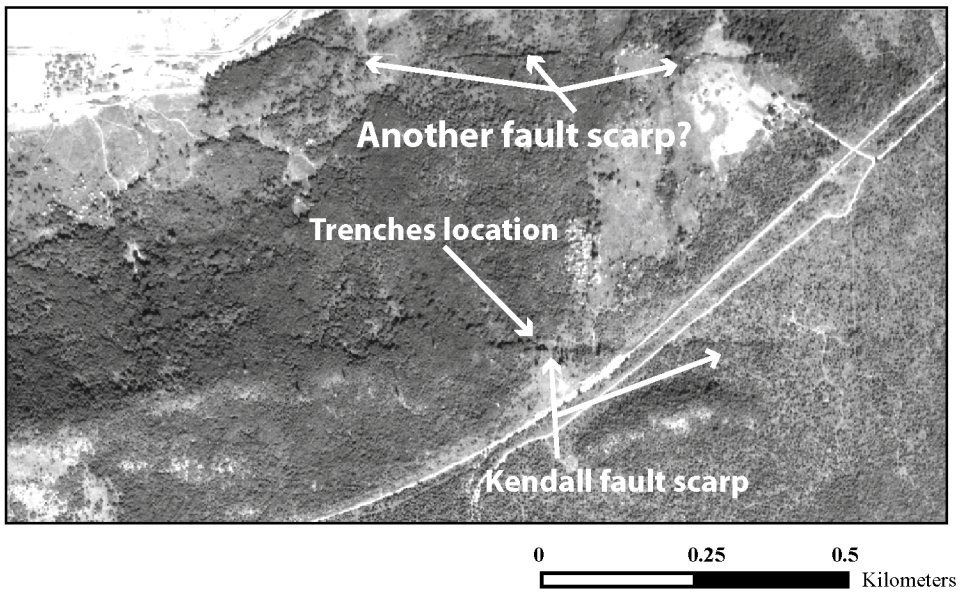

Figure 17: A possible second fault scarp located 0.5 km north of the Kendall fault scarp. Orthophotograph compiled from 1933 Seattle district Army Corps of Engineers aerial photos. B. Kendall scarp shown by LiDAR.

Knowing not only how many active strands exists, but what is the extent of faulting along a possibly reactivated Boulder Creek fault would be important to seismic hazards assessments. The Boulder Creek fault is mapped as a ~20 km long structure, not including the Smith Creek fault. Is only the Nooksack portion active or can the entire fault rupture? Would it rupture at once or in segments? Could the Smith Creek and Macauley Creek faults have been recently active, as Dragovich et al. (1997b) suggest? Does the Boulder Creek fault extend farther west into the Puget Lowlands? These are the kind of questions that should prompt continued work in the Kendall fault scarp and Boulder Creek area.

CONCLUSION

Trench and wetland coring studies of the newly recognized Kendall fault scarp document late Holocene faulting at the northeast margin of the Puget Sound. The earliest of the three earthquakes recorded in the trenches and the adjacent wetland occurred shortly before ~7700 yr BP and folded the scarp but did not produce surface faulting. In the two most recent earthquakes, a shallow-dipping north-verging reverse fault thrust glacial outwash over Holocene soils. The timing of the two most recent earthquakes is ~3000 and ~900 yrs BP respectively, as indicated by radiocarbon samples taken from the trench and wetland buried soils.

The structural setting of the Kendall fault scarp is paradoxical in that the fault trace of reverse slip documented in the trenches trends along and is located within 500 m of a bedrock normal fault, the Boulder Creek fault. Although the Boulder Creek fault previously was interpreted to be inactive since the early Tertiary, the Kendall fault scarp may result from reverse faulting along a strand of the Boulder Creek fault reactivated as a thrust fault accommodating north-south contraction of western Washington.

REFERENCES CITED

Armstrong, J.E.,Crandell, D.R., Easterbrook, D.J., and Noble, J.B., 1965, Late Pleistocene stratigraphy and chronology in the southwestern British Columbia and northwestern Washington: Geological Society of America Bulletin, v. 76, p, 321-330.

Atwater, B.F. and Moore, A.L., 1992, A tsunami about 1000 years ago in Puget Sound, Washington: Science, v. 258, p. 1614-1617.

Bacon, C.R., and Lanphere, M.A., 2006, Eruptive history and geochronology of Mount Mazama and the Crater Lake region, Oregon: Geological Society of America Bulletin, v. 118, p.1331-1359.

Blakely, R.J., 1995, Potential theory in gravity and magnetic applications, Cambridge Unversity Press, 441 p.

Blakely, R.J., Wells, R.E., and Weaver, C.S., 1999, Puget Sound aeromagnetic maps and data: U.S. Geological Survey Open-File Report 99-514, http://geopubs.wr.usgs.gov/open-file/of99-514.

Blakely, R.J., Wells, R.E., Weaver, C.S., and Johnson, S.Y., 2002, Location, structure, and seismicity of the Seattle fault zone, Washington: Evidence from aeromagnetic anomalies, geologic mapping, and seismic-reflection data: Geological Society of America Bulletin, v. 114, p. 169-177.

Blakely, R.J., Sherrod, B.L., Wells, R.E., Weaver, C.S., McCormack, D.H., Troost, K.G., and Haugerud, R.A., 2004, The Cottage Lake aeromagnetic lineament: A possible

onshore extension of the southern Whidbey Island fault, Washington: U.S. Geological Survey Open File Report 2004-1204, 60 p.

Brocher, T.M., Blakely, R.J., and Wells, R.E., 2004, Interpretation of the Seattle Uplift, Washington, as a passive-roof duplex: Bulletin of the Seismological Society of America, v. 94, p. 1379-1401.

Brown, E.H., 1987, Structural geology and accretionary history of the Northwest Cascades System, Washington and British Columbia: Geological Society of America Bulletin, v. 99, p. 201-214.

Bucknam, R.C., Hemphill-Haley, E., and Leopold, E.B., 1992, Abrupt uplift within the past 1,700 years at southern Puget Sound, Washington: Science, v. 258. p. 1611-1614.

Clague, J.J., Mathewes, R.W., Guilbault, J.P., Hutchinson, I., and Ricketts, B.D., 1997, Pre-Younger Dryas resurgance of the wouthwestern margin of the Cordilleran ice sheet, British Columbia, Canada: Boreas, v.26, p. 261-278.

Dragovich, J.D., Norman, D.K., Haugerud, R.A., and Pringle, P.T., 1997a, Geologic Map and Interpreted Geologic History of the Kendall and Deming 7.5-minute Quadrangles, western Whatcom County, Washington, Washington Division of Geology and Earth Resources, Open-File Report 97-2, 39 p.

Dragovich, J.D., Zollweg, J.E., Qamar, A.I., and Norman, D.K., 1997b, The Macaulay Creek thrust, the 1990 5.2-magnitude Deming earthquake, and Quaternary geologic anomalies in the Deming area, Western Whatcom County, Washington - cause and effects?: Washington Geology, v. 25, p. 15-27.

Dragovich, J., 2006, written communication

Finn, C., Phillips, W.M., and Williams, D.L., 1991, Gravity anomaly and terrain maps of Washington: U.S. Geological Survey Geophysical Investigations Map, GP-988, scale 1:500,000 and 1:1,000,000.

Foit, F., 2006, written communication

Haugerud, R.A., Harding, D.J., Johnson, S.Y., Harlesss, J.L., and Weaver, C.S., 2003, High resolution lidar topography of the Puget Lowland, Washington- A bonanza for earth science: GSA Today, v. 13, p. 4-10.

Haugerud, R.A., Sherrod, B.L., Wells, R.E., and Hyatt, T., 2005, Holocene displacement on the Boulder Creek fault near Bellingham, Washington, and implications for kinematics of deformation of the Cascadia forearc: Abstracts with Programs, Geological Society of America, v. 37, p. 476.

Haugerud, R.A., 2006, written communication

Hughes, J., 2006, written communication

Hyndman, R.D., Mazzotti, S., Weichert, D., and Rogers, G.C., 2003, Frequency of large crustal earthquakes in Puget Sound-Southern Georgia Strait predicted from geodetic and geological deformation rates: Journal of Geophysical Research, B, Solid Earth and Planets, v.108, 12 p.

Johnson, S.Y., 1982, Stratigraphy, sedimentology, and tectonic setting of the Eocene Chuckanut Formation, Northwest Washington: University of Washington Docotor of Philosophy Thesis, 221 p., 4 plates.

Johnson, S.Y., Potter, C.J., Armentrout, J.M., Miller, J.J., Finn, C, and Weaver, C.S., 1996, The southern Whidbey Island fault: An active structure in the Puget Lowland, Washington: Geological Society of America Bulletin, v. 108, no. 3, p. 334-354.

Johnson, S.Y., Dadisman, S.V., Childs, J.R., and Stanley, W.D., 1999, Active tectonics of the Seattle fault and central Puget Sound, Washington: Implications for earthquake hazards: Geological Society of America Bulletin, v. 111. p. 1042-1053.

Johnson, S.Y., Dadisman, S.V., Mosher, D.C., Blakely, R.J., and Childs, J.R., 2001, Active tectonics of the Devils Mountain fault and related structures, northern Puget Lowland and eastern Strait of Juan de Fuca region, Pacific Northwest: U.S. Geological Survey Professional Paper 1643, 45 p., 2 plates.

Johnson, S.Y., Nelson, A.R., Personius, S.F., Wells, R.E., Kelsey, H.M., Sherrod, B.L., Okumura, K., Koehler, R., Witter, R.C., Bradley, L., and Harding, D.J., 2004, Evidence for late Holocene earthquakes on the Utsalady Point fault, northern Puget Lowland, Washington: Bulletin of the Seismological Society of America, v. 94, p. 2299-2316.

Kelsey, H.M., Sherrod, B.L., Johnson, S.Y., and Dadisman, S.V., 2004, Land-level changes from a late Holocene earthquake in the northern Puget Lowland, Washington: Geology, v. 32, p. 469-472.

Kovanen, D.J., 1996, Extensive late-Pleistocene alpine glaciation in the Nooksack River Valley, North Cascades, Washington: Western Washington University Master of Science Thesis, 186 p.

Kovanen, D.J., Easterbrook, D.J., 2001, Late Pleistocene, post-Vashon, alpine glaciation of the Nooksack drainage, North Cascades, Washington: Geologic Society of America Bulletin, v. 113, p. 274-288.

Lidke, D.J., Johnson, S.Y., McCrory, P.A., Personius, S.F., Nelson, A.R., Dart, R.L., Bradley, L., Haller, K.M., and Machette, M.N., 2003, Map and data for Quaternary faults and folds in Washington state: U.S. Geological Survey Open-File Report 03-428, 15 p., 1 sheet.

Mazzotti, S., Dragert, H., Hyndman, R.D., Miller, M.M., and Henton, J.A., 2002, GPS deformation in a region of high crustal seismicity: N. Cascadia forearc: Earth and Planetary Science Letters, v. 198, p. 41-48.

Misch, P., 1966, Tectonic evolution of the northern Cascades of Washington State - A Cordilleran case history: in Symposium on tectonic history and mineral deposits in the Western Cordillera of British Columbia and neighboring United States, Canadian Institute of Mining and Metallurgy, Special Volume 8, p. 101-148.

Misch, P., 1977, Bedrock geology of the North Cascades, in Brown, E.H., and Ellis, R.C., eds., Geological excursions in the Pacific Northwest, GSA 1977 Annual Meeting Guidebook, Field Trip No. 1, Western Washington University Press.

Moen, W.S., 1962, Geology and mineral deposits of the northern half of the Van Zandt quadrangle, Whatcom County, Washington: Division of Mines and Geology Bulletin No. 50, 129 p., 4 plates.

Nelson, A.R., Johnson, S.Y., Kelsey, H.M., Wells, R.E., Sherrod, B.L., Pezzopane, S.K., Bradley, L., Koehler, R.D., and Bucknam, R.C., 2003, Late holocene earthqaueks on the Toe Jam Hill fault, Seattle fault zone, Bainbridge Island, Washington: Geological Society of America Bulletin, v. 115, p. 1388-1403.

Pacific Northwest Seismic Network, 2006: http://www.pnsn.org/CATDAT/welcome.html

Pratt, T.L., Johnson, S.Y., Stephenson, W., and Finn, C., 1997, Seismic reflection images beneath Puget Sound, western Washington state: the Puget Lowland thrust sheet hypothesis: Journal of Geophysical Research, v. 102, p. 27,469-27,489.

Saad, A.F., 1969, Magnetic properties of ultramafic rocks from Red Mountain, California: Geophysics, v. 34, p. 974-987.

Schoeneberger, P.J., Wysocki, D.A., Benham, E.C., and Broderson, W.D., eds., 2002, Field book for describing and sampling soils, Version 2.0: Natural Resources Conservation Service, National Soil Survey Center Lincoln, NE.

Sherrod, B.L., 2001, Evidence for earthquake-induced subsidence about 1100 years ago in coastal marshes of southern Puget Sound, Washington: Geological Society of America Bulletin, v. 113, p. 1299-1311.

Sherrod, B.L., Brocher, T.M., Weaver, C.S., Bucknam, R.C., Blakely, R.J., Kelsey, H.M., Nelson, A.R., and Haugerud, R., 2004, Holocene fault scarps near Tacoma, Washington, USA: Geology, v. 32, p. 9–12.

Sherrod, B.L., Blakely, R.J., Weaver C.S., Kelsey, H., Barnett, E., and Wells, R., 2005, Holocene fault scarps and shallow magnetic anomalies along the SWIF Zone near Woodinville, Washington: USGS Open File Report 2005-1136, 35 p.

Sherrod, B.L., 2006, written communication.

Stuiver, M., and Reimer, P.J., 1993, Extended 14C database and revised CALIB radiocarbon calibration program: Radiocarbon, v.35, p. 215-230.

Stuiver, M., Reimer, P.J., and Reimer, R.W., 2005, CALIB 5.0 [http://calib.qub.ac.uk/calib/ program and documentation]

Tabor, R.W., Haugerud, R.A., Booth, D.B., and Brown, E.H., 1994, Preliminary geologic map of the Mount Baker 30- by 60- minute quadrangle, Washington: U.S. Geological Survey Open-File Report 94-403, p. 55, 2 pl.

Tabor, R.W., Frizzell, V.A., Jr., Booth, D.B., and Waitt, R.B., 2000, Geologic map of the Snoqualmie Pass 30' by 60' quadrangle, Washington: U.S. Geology Survey Miscellaneaous Investigations Series Map I-2538, scale 1:100,000.

Tabor, R.W., Haugerud, R.A., Hildreth, W., and Brown, E.H., 2003, Geologic Map of the Mount Baker 30- by 60-minute quadrangle, Washington: U.S. Geologic Survey, Report I-2660, 74 p., 2 sheets.

Walsh, T.J., Logan, R.L., and Neal, K.G., 1997, The Canyon River fault, an active fault in the southern Olympic Range, Washington, Washington Geology, v. 25, p. 21-24.

Wells, R.E., Weaver, C.S., and Blakely, R.J., 1998, Forearc migration in Cascadia and its neotectonic significance: Geology, v. 26. p. 759-762.

Wells, R.E. and Simpson, R.W., 2001, Northward migration of the Cascadia forearc in the northwestern U.S. and implications for subduction deformation: Earth, Planets, and Space, v.53, p. 275-283.

Wilson, J.R., Bartholomew, M.J., and Carson, R.J., 1979, Late Quaternary faults and their relationship to tectonism in the Olympic Peninsula, Washington: Geology, v. 26, p. 235-239.

Witter, R.C., Givler, R.W., Zeliff, M., Iacoboni, C., and Carson, R.J., 2006, Two post-glacial earthquakes on the Saddle Mountain West fault, southeastern Olympic Peninsula, Washington: U.S. Geological Survey, National Earthquake Hazard Reduction Program Final Report, 42 p., 2 plates.

Zdanowicz, C.M., Zielinski, G.A., and Germani, M.S., 1999, Mount Mazama eruption: Calendrical age verified and atmospheric impact assessed: Geology, v. 27, p. 621-624.